PB 161554

NBS

Technical Note No. 53

Boulder Laboratories

CARRIER FREQUENCY DEPENDENCE OF THE BASIC TRANSMISSION LOSS IN TROPOSPHERIC FORWARD SCATTER PROPAGATION

BY KENNETH A. NORTON

U. S. DEPARTMENT OF COMMERCE
NATIONAL BUREAU OF STANDARDS

THE NATIONAL BUREAU OF STANDARDS

Functions and Activities

The functions of the National Bureau of Standards are set forth in the Act of Congress, March 3, 1901, as amended by Congress in Public Law 619, 1950. These include the development and maintenance of the national standards of measurement and the provision of means and methods for making measurements consistent with these standards; the determination of physical constants and properties of materials; the development of methods and instruments for testing materials, devices, and structures; advisory services to government agencies on scientific and technical problems; invention and development of devices to serve special needs of the Government; and the development of standard practices, codes, and specifications. The work includes basic and applied research, development, engineering, instrumentation, testing, evaluation, calibration services, and various consultation and information services. Research projects are also performed for other government agencies when the work relates to and supplements the basic program of the Bureau or when the Bureau's unique competence is required. The scope of activities is suggested by the listing of divisions and sections on the inside of the back cover.

Publications

The results of the Bureau's work take the form of either actual equipment and devices or published papers. These papers appear either in the Bureau's own series of publications or in the journals of professional and scientific societies. The Bureau itself publishes three periodicals available from the Government Printing Office: The Journal of Research, published in four separate sections, presents complete scientific and technical papers; the Technical News Bulletin presents summary and preliminary reports on work in progress; and Basic Radio Propagation Predictions provides data for determining the best frequencies to use for radio communications throughout the world. There are also five series of nonperiodical publications: Monographs, Applied Mathematics Series, Handbooks, Miscellaneous Publications, and Technical Notes.

Information on the Bureau's publications can be found in NBS Circular 460, Publications of the National Bureau of Standards ($1.25) and its Supplement ($1.50), available from the Superintendent of Documents, Government Printing Office, Washington 25, D.C.

NATIONAL BUREAU OF STANDARDS
Technical Note
53

May 12, 1960

CARRIER FREQUENCY DEPENDENCE OF THE BASIC TRANSMISSION LOSS IN TROPOSPHERIC FORWARD SCATTER PROPAGATION

by

Kenneth A. Norton

NBS Technical Notes are designed to supplement the Bureau's regular publications program. They provide a means for making available scientific data that are of transient or limited interest. Technical Notes may be listed or referred to in the open literature. They are for sale by the Office of Technical Services, U. S. Department of Commerce, Washington 25, D. C.

DISTRIBUTED BY

UNITED STATES DEPARTMENT OF COMMERCE
OFFICE OF TECHNICAL SERVICES
WASHINGTON 25, D. C.

Price $ 1.00

FOREWORD

Essentially this same paper, but omitting Tables III and IV, will be published in the July, 1960 issue of the Journal of Geophysical Research. The primary purpose of this additional publication is to provide Tables III and IV.

Carrier Frequency Dependence of the Basic Transmission Loss in Tropospheric Forward Scatter Propagation

by

Kenneth A. Norton

Summary

A further interpretation is given of certain Lincoln Laboratory data obtained in an experiment using scaled antennas as presented in a recent letter to the Proceedings of the I.R.E. from Bolgiano.[1/] This paper has four objectives: first, to clarify the significance of these data from the standpoint of the engineer developing long-range tropospheric scatter systems; second, to apply a further statistical analysis to these data; third, to consider their significance as regards the theory of radio propagation through a turbulent atmosphere; and fourth, to describe a suitable method for the measurement of the meteorological parameters entering the theory. Based on this analysis of the Lincoln Laboratory data, it is concluded that the carrier frequency dependence of the basic transmission loss cannot be variable from hour to hour.

1. Significance of the Lincoln Laboratory Experiment to the Systems Engineer

From the standpoint of the development of a forward scatter communications system, the radio engineer is usually interested in the cumulative distribution of the hourly median basic transmission loss [2] (sometimes called path loss) over as long a period of time as is feasible, and he usually bases the power required for a specified performance on the expected path antenna power gain, together with the basic transmission loss which is not exceeded for more than some large percentage of the hours, say 99% or 99.9%. Fig. 1 shows the cumulative distributions of basic transmission loss for 417 Mc and 2290 Mc, and these are based on the same 240 pairs of hourly median values used by Bolgiano for determining the results shown on Fig. 1 of his letter. [1] J. H. Chisholm and J. F. Roche of Lincoln Laboratory supplied the 480 values of available power, P_a, in decibels above one watt at the terminals of the receiving antenna, and these were converted to basic transmission losses by means of the formula $L_b = P_t - P_a + G_p - L_t - L_r$ where P_t is the transmitter power in decibels above one watt, G_p is the path antenna gain, and L_t and L_r are line losses. On 417 Mc we set $P_t = 35.4$ db, $L_t + L_r = 1.1$ db, $G_p = 56.2$ db, and on 2290 Mc we set $P_t = 40$ db, $L_t + L_r = 2.1$ db, $G_p = 61.2$ db; the path antenna gain was estimated by Hartman and Wilkerson's method [3] to be 0.8 db below the sum of the free space gains for both frequencies.

By examining a large number of cumulative distributions such as those shown on Fig. 1 for 80 different scatter paths and

DATA FROM THE LINCOLN LABORATORY EXPERIMENT
February 11 to July 11, 1957

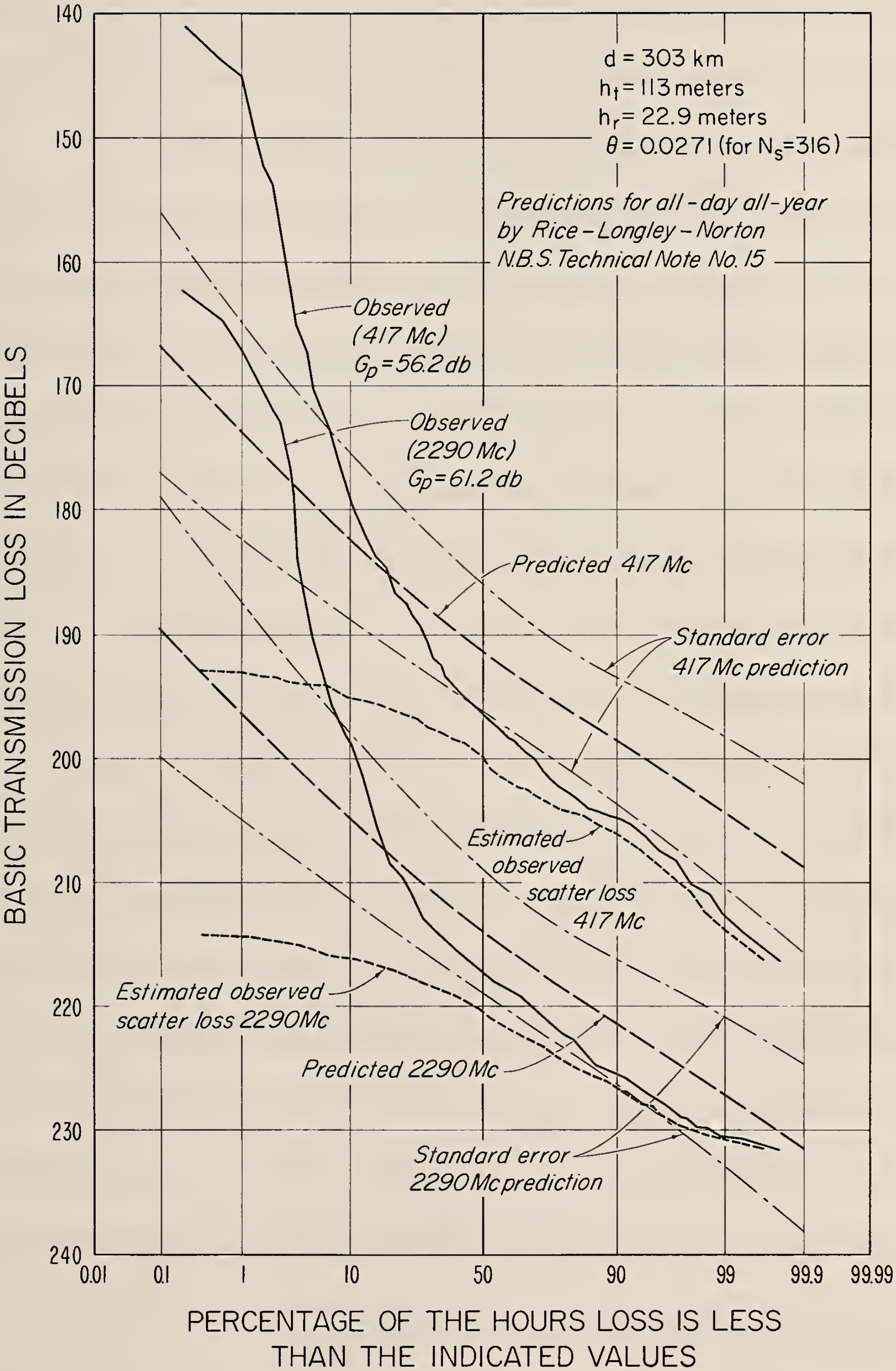

Figure 1

involving a range of frequencies from 66 Mc to 1046 Mc, Norton, Rice and Vogler [4/] found, after correcting by means of a frequency gain function for the incomplete illumination of the lower part of the common volume on the lower frequencies, that the basic transmission loss for the scatter mode of propagation increases with frequency as $(29.56 \pm 2.44) \log_{10}(f_2/f_1)$; these results were obtained on the assumption that the scattering cross section decreases inversely as the square of the height above the surface. More recently, Rice, Longley and Norton [5/] have found, on the presumably more realistic assumption that the scattering cross section decreases exponentially with the height above the surface, that the basic transmission loss for the scatter mode of propagation increases with frequency, after adjustment by means of the frequency gain function, as $(33.1 \pm 5.55) \log_{10}(f_2/f_1)$; this latter determination involved 105 scatter paths covering the range of frequencies from 66 Mc to 4090 Mc.* Since the frequency dependence expected on the basis of those mixing-in-gradient hypotheses developed in several recent papers [6/] [7/] [8/] is $30 \log_{10}(f_2/f_1)$ and since this lies well within the error bands of the above experimental determinations, it has been common practice for engineers in recent years to use this theoretical frequency dependence for estimating the basic transmission loss expected on a scatter path. In this connection it appears that the

* A further discussion is given in Appendix III.

formula for the basic transmission loss given by Rice, Longley and Norton [5/] for an exponential atmosphere, when used in conjunction with the Hartman and Wilkerson [3/] formula for the path antenna gain, is the most versatile formula presently available for determining the transmission loss expected on a given path since it makes allowance for the effects of irregularities in the terrain, and may be used for essentially any antenna heights, radio frequencies or geographical locations. The cumulative distributions of basic transmission loss as predicted by this formula are shown on Fig. 1, together with their standard errors, and these are evidently in reasonably good agreement with the observed losses; the standard error of predicting the median using this formula is about 5 db, and the observed medians indicate less than 6 db more loss than the predicted medians on both frequencies. A part of this difference may be due to the fact that our prediction is for an all-day, all-year period, while the data were obtained in a period from February 11 to July 11, 1957. A more likely explanation of this small error of prediction is some random effect of this particular terrain profile since our formula makes use only of the angular distance in allowing for the effects of the terrain. Our prediction for this path is evidently not very good for the smaller losses which occur for small percentages of the hours, and further work is now in progress on improving our methods of prediction of these smaller losses since this portion of the cumulative distribution, although not important for predicting the effective range of systems in the absence of interference, is important for the prediction of the interference expected between systems.

2. A Further Statistical Analysis

For percentages of the hours less than about 30%, it appears that modes of propagation other than, or in combination with, scatter were probably involved on the Lincoln Laboratory path--possibly ducts or well defined elevated layers; the smallest observed values exceed the expected loss in free space by only 7.3 db on 417 Mc and 13.6 db on 2290 Mc, and such small losses undoubtedly cannot be attributed exclusively to the scatter mode of propagation.

Since it appears on Fig. 1 that the stronger fields (smaller basic transmission losses) probably did not arrive at the receiving location via the simple scatter mode of propagation, it will be well to eliminate these from the analysis which will now be made for the purpose of better understanding the physical nature of the scatter mode of propagation. This was accomplished somewhat arbitrarily simply by including only those pairs of hourly medians for which the basic transmission losses were greater than 192.3 db on 417 Mc, and simultaneously greater than 214.3 db on 2290 Mc; in this way we

APPARENT VARIATION OF μ FROM THE LINCOLN LABORATORY EXPERIMENT

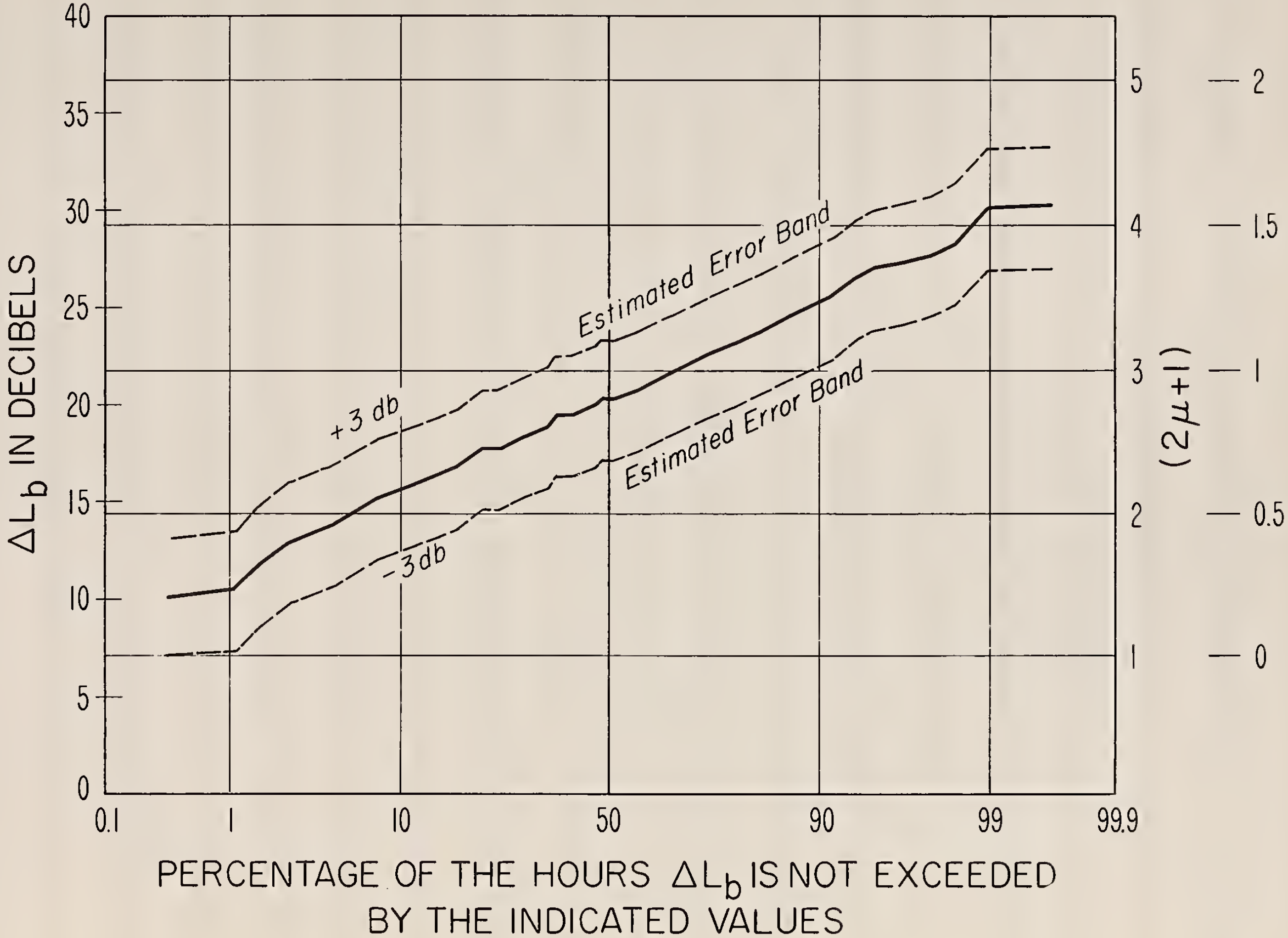

Figure 2

obtained a reduced sample of only 140 pairs of hourly medians which are clearly more nearly representative of the pure scatter mode of propagation. The cumulative distributions of these values are also shown on Fig. 1. We next obtained the means and standard deviations from these samples: $\overline{L}_b(417) = 200.5$ db; $\sigma(417) = 4.65$ db; $\overline{L}_b(2290) = 221.0$ db; $\sigma(2290) = 4.06$ db; $\rho = 0.63$; here ρ denotes the correlation coefficient between the basic scatter transmission losses for 417 and 2290 Mc. Next we determined the cumulative distribution of the differences of these 140 pairs of scatter losses $\Delta L_b \equiv L_b(2290) - L_b(417)$; this distribution is shown on Fig. 2, and the mean and standard deviations were found to be: $\overline{\Delta L_b} = 20.5$ db and $\sigma(\Delta L_b) = 3.79$ db. Bolgiano's ΔL was actually not a difference in basic transmission losses, although his label on his Fig. 1 indicates that it was; however, his wavelength scale is consistent with the assumption that his ΔL is the difference in losses relative to free space, and presumably this is what he plotted. The calculated frequency gain corresponded to an additional loss of 0.5 db on 417 Mc and to 0 db on 2290 Mc; after making allowance for this difference, our analysis using only the above scatter losses <u>appears</u> to indicate a variation in the wavelength dependence exceeding $34.9 \log_{10}(2290/417)$ for 10% of the hours, exceeding $28.3 \log_{10}(2290/417)$ for 50% of the hours, and exceeding $22.0 \log_{10}(2290/417)$ for 90% of the hours.

We are now in a position to ask the question whether this apparent variation in the wavelength dependence of the scatter loss from hour to hour represents a real change in the physical nature of the atmosphere from hour to hour. In this connection it should be noted that the hourly medians on closely adjacent paths, such as are used for diversity reception, and involving the <u>same</u> radio frequency, are not perfectly correlated [9/] and the correlation appears to be substantially smaller when the antennas used on the two adjacent paths have different radiation characteristics. Thus it appears that the correlation coefficient is very dependent upon whether the two antennas illuminate exactly the same portions of the atmosphere. Thus Barsis [9/] found at 100 Mc that the hourly median values of L_b over 644 km scatter paths using Yagi and Rhombic receiving antennas separated normal to the path by only 18 meters were very poorly correlated; with the transmitter at Fort Carson, the angular distance* to the two receiving antennas was 0.068 radians, and the correlation between L_b(Yagi) and L_b(Rhombic) was $\rho = 0.510$, whereas with the transmitter at Cheyenne Mountain, the angular distance to the same two receiving antennas was 0.0585, and the correlation $\rho = 0.331$. The observed standard deviations of $\Delta L_b = L_b$ (Yagi) - L_b (Rhombic) were $\sigma(\Delta L_b$ for $\theta = 0.068) = 1.61$ db and $\sigma(\Delta L_b$ for $\theta = 0.0585) = 2.48$ db. The angular distance for the Lincoln

* The definition of the angular distance, θ, is given on Fig. 3.

Laboratory path is approximately $\theta = 0.0271$, and it is thus not surprising that $\sigma(\Delta L_b)$ was observed on this path to be somewhat larger. Although the free space radiation patterns of the antennas used for the Lincoln Laboratory experiments were very nearly identical, the antennas on the two frequencies nevertheless did not illuminate the same portions of the atmosphere since they were located at different numbers of wavelength above the ground, and thus had markedly different vertical plane lobe structures. It is believed that this may be the correct explanation for at least some if not all of the observed variance $\sigma(\Delta L_b) = 3.79$ db rather than any change in the scattering nature of the atmosphere from hour to hour. It would be most interesting to repeat the Lincoln Laboratory experiment under conditions which would ensure that more nearly the same portion of the atmosphere is illuminated by the antennas on the two frequencies. Although the writer has been unable to devise an experimental plan which will ensure that exactly the same portion of the atmosphere is involved, the following experimental arrangement would appear to approximate this situation reasonably well: (1) choose a scatter path with extremely flat terrain (possibly calm fresh water lakes) in the foregrounds of the antennas so that the vertical plane lobe structures will be well defined on both frequencies, (2) use parabolic antennas with the same diameters expressed in wavelengths, i.e., with the same apertures, (3) erect the antennas at approximately the same heights expressed in wavelengths above the ground in such a way that the lowest lobes, having regard to the curvature of the earth, are very nearly coincident on the two frequencies throughout the scattering volume, (4) keep the spacing between the antennas normal to the path at a minimum and (5) have the lower frequency antennas to the right of the higher frequency antennas when facing the far terminal so that the two propagation paths will cross in the middle of the scattering volume. With such an experimental arrangement the only significant difference in the portions of the atmosphere involved in the propagation on the two frequencies will be found near the transmitting and receiving ends of the path; to provide a measure of the importance of such effects, a control path could be added using a slightly different low frequency with its terminals to the left of the higher frequency antennas. It would be interesting to carry out such an experiment, and it is anticipated that the correlation ρ would then be very much nearer to unity and $\sigma(\Delta L_b)$ substantially smaller.

3. A Theoretical Interpretation

Finally it is of interest, in spite of the above questions raised as to the appropriateness of these data for this purpose, to assume that all of the apparent variation in the above-described frequency dependence does actually represent real physical changes in the characteristics of the atmosphere from hour to hour and to speculate on the nature of these changes. Assuming that the scattering occurs in a turbulent atmosphere, it is well known 8/ 10/ that the power scattered per unit volume is proportional to the magnitude $S(\vec{k})$ of the three dimensional wave-number spectrum of the variations of the refractive index of the atmosphere at a fixed instant of time and corresponding to the particular wave number $\vec{k} \equiv (2\pi/\ell)\,\vec{k}_1$, where the scale length $\ell = \lambda/2 \sin[(\alpha + \beta)/2] \cong \lambda/(\alpha + \beta)$ and $\vec{k}_1$ is a unit vector. Here λ denotes the free space wavelength of the scattered radio waves and--see Fig. 3--$(\alpha + \beta)$ is the scattering angle in the scattering plane, i.e., the plane passing through the transmitting antenna, receiving antenna and the elementary scattering volume. The wave number spectrum is determined in each elementary scattering volume for that direction $\vec{k}_1$ which is in the scattering plane and is normal to the line which bisects the angle $(\alpha + \beta)$. The total power scattered is obtained by integrating $S[2\pi(\alpha + \beta)/\lambda, \vec{k}_1]$ for these appropriate directions $\vec{k}_1$ throughout the scattering volume; $\vec{k}_1$ tends to be vertical throughout those portions of the scattering volume from which the scattering is most intense. Note that the angular distance, θ, is the minimum value which $(\alpha + \beta)$ may have within the important common volume, i.e., that portion of the scattering volume which is within line-of-sight of both the transmitting

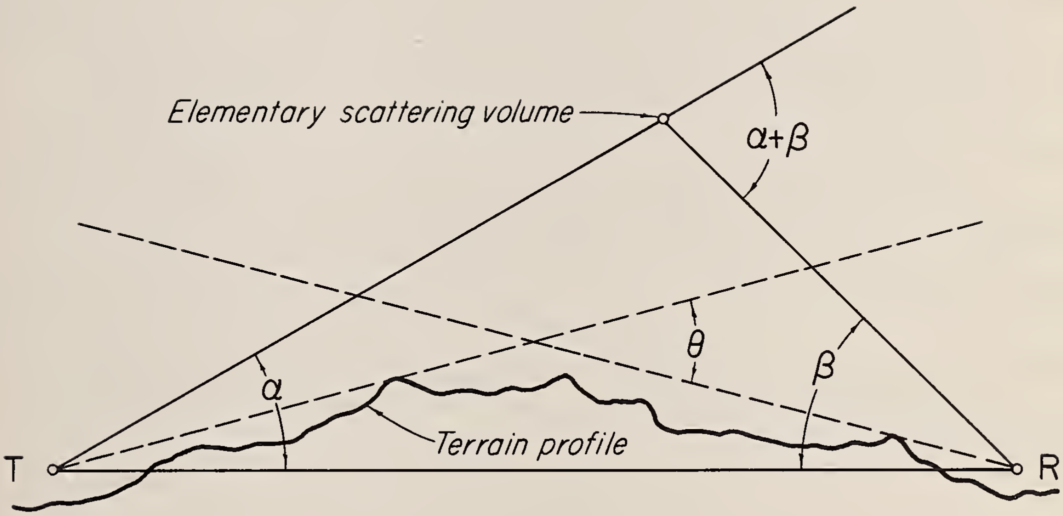

FIG. 3 DEFINITION OF THE ANGULAR DISTANCE θ
AND THE SCATTERING ANGLE $(\alpha + \beta)$

and receiving antennas. Table I gives the values of $\ell_{max} = \lambda/\theta$ and of $\ell_{min} = \lambda/0.2$ (assuming that negligible scatter is expected for $(\alpha + \beta) > 0.2$ radians) for a wide range of frequencies and angular distances; the distance $d_s = a\theta$ between the horizons of the transmitting and receiving antennas is also given on the assumption that the effective earth's radius, a, is equal to 9,000 kilometers which corresponds, for a typical CRPL exponential atmosphere, [11] to a surface refractivity of $N_s = (n_s - 1)\cdot 10^6 \cong 316$ and this latter value is roughly the average value of N_s throughout the day and over the continental United States.

Table I

Ranges of Scales Pertinent to the Forward Scatter of Radio Waves

	$\theta = 0.005$ $d_s = 45$ km	$\theta = 0.025$ $d_s = 225$ km	$\theta = 0.05$ $d_s = 450$ km	$\theta = 0.1$ $d_s = 900$ km	$(\alpha + \beta) = 0.2$
f_{Mc}	ℓ_{max} meters	ℓ_{max} meters	ℓ_{max} meters	ℓ_{max} meters	ℓ_{min} meters
50	1200	240	120	60	30
100	600	120	60	30	15
200	300	60	30	15	7.5
500	120	24	12	6	3
1000	60	12	6	3	1.5
2000	30	6	3	1.5	0.75
5000	12	2.4	1.2	0.6	0.3
10000	6	1.2	0.6	0.3	0.15

For the Lincoln Laboratory path ℓ_{max} = 26.5 meters on 417 Mc and ℓ_{max} = 4.8 meters on 2290 Mc, and thus only that portion of the wave-number spectrum of tropospheric turbulence with wave-numbers k greater than $2\pi/\ell_{max}$ will be involved in the scattering. Assuming that the scattering occurs primarily from the common volume lying above the two surfaces generated by the two horizon rays, it will occur on the Lincoln Laboratory path at heights above the ground in excess of approximately $a\theta^2/8$ = 0.826 kilometers.

The average scattered power, p_s, available at a given time from the receiving antenna for a given power, p_t, radiated from the transmitting antenna is expected to depend on the free space wavelength in the following way:

$$(p_s/p_t) \sim \lambda^{-4} \cdot \int g_t\, g_r\, S[2\pi(\alpha + \beta)/\lambda,\ \vec{k}_1]\, dv \cdot \lambda^2 \qquad (1)$$

The first factor λ^{-4} in (1) may be identified with the Rayleigh law of uniform scattering in all directions from small scatterers; the second factor is an integral throughout the scattering volume which properly corrects the Rayleigh scattering law to allow for the tendency with <u>large</u> scatterers for the power to be scattered primarily in the forward direction; finally the factor λ^2 allows for the fact that the available power from a receiving antenna is equal to $\lambda^2 g_r/4\pi$ times the scattered power flux density. A factor $\sin^2 \chi \cong 1$ which allows for the small effects of polarization has been omitted under the integral sign in (1); g_t and g_r in (1) denote the effective power gains of the transmitting and receiving antennas at the elementary scattering volume, dv, relative to an isotropic antenna including the effects of ground reflection, e.g., g_t could in principle be measured as the ratio of the power flux densities at dv when the actual antenna and the earth are replaced by an isotropic antenna in free space at the same distance.

The instantaneous received power, p_i, is Rayleigh distributed about the mean value $< p_s >$:

$$Q(p_i > y) = \exp(-y/<p_s>) \tag{2}$$

Q is the probability that the instantaneous power p_i exceeds some given value y. The Lincoln Laboratory experiment was reported in terms of hourly median powers, p_m, and these hourly medians are, on the assumption of the Rayleigh distribution, related to p_s by $p_m = (\log_e 2) < p_s >$ where $< p_s >$ is the time average of p_s over a period of one hour. Since the values of ΔL were differences of hourly medians, we see by (1) that ΔL is given by:

$$\Delta L = 10 \log_{10} \left[\frac{< \int g_{t_1} g_{r_1} S[2\pi(\alpha+\beta)/\lambda_1, \vec{k}_1]\, dv >}{< \int g_{t_2} g_{r_2} S[2\pi(\alpha+\beta)/\lambda_2, \vec{k}_1]\, dv >} \right] - 20 \log_{10}(f_2/f_1) \tag{3}$$

It appears from (3) that variations of ΔL from hour to hour may only be explained in terms of variations in the above integrations over space and subsequent averages with respect to time and thus, to the extent that the transmitting and receiving antennas actually "see" the same common volume on the two frequencies, i.e., $g_{t_1} = g_{t_2}$ and $g_{r_1} = g_{r_2}$ throughout the scattering volume, it appears that ΔL would be expected to vary only if the shape of the wave-number spectrum varies from hour to hour.

Unfortunately there does not appear to be any exact way to measure $S(\vec{k})$ directly so that it must be determined indirectly as the Fourier cosine space transform of a correlation function $C(\vec{r})$:

$$S(\vec{k}) \equiv V_n \iiint d^3\vec{r}\, \cos[\vec{k}\cdot\vec{r}]\, C(\vec{r}) \tag{4}$$

$$C(\vec{r}) = \frac{<\Delta n(\vec{R})\cdot\Delta n(\vec{R}+\vec{r})>}{\{<[\Delta n(\vec{R})]^2><[\Delta n(\vec{R}+\vec{r})]^2>\}^{1/2}} \tag{5}$$

where $< >$ denotes as before a time average over a short period of, say one hour, $\Delta n(\vec{R})$ and $\Delta n(\vec{R}+\vec{r})$ denote the measured changes in the refractive indices of the atmosphere from their mean values $<n(\vec{R})>$ and $<n(\vec{R}+\vec{r})>$ at the vector locations $\vec{R}$ and $\vec{R}+\vec{r}$. In what follows we will assume homogeneous turbulence, and then $C(\vec{r})$ depends only on the magnitude and direction of $\vec{r}$ and $<[\Delta n(\vec{R})]^2> = <[\Delta n(\vec{R}+\vec{r})]^2> \equiv V_n$. The following model correlation function has proved to be useful [10/ 14/ 15/]

for characterizing the random deviations of n at least over the range of $r < \ell_o$:

$$C(\vec{r}) = \{2^{1-\mu}/\Gamma(\mu)\}(r/\ell_o)^{\mu} K_{\mu}(r/\ell_o) \tag{6}$$

In the above, Γ denotes a gamma function, K_μ denotes the modified Bessel function of the second kind and μ is a constant. Some allowance for the possible effects of anisotropy has been introduced into (6) by allowing the characteristic scale ℓ_o to vary with the direction of $\vec{r}$:

$$\frac{1}{\ell_o^2} = \frac{\cos^2\phi}{\ell_v^2} + \sin^2\phi\left[\frac{\cos^2\gamma}{\ell_p^2} + \frac{\sin^2\gamma}{\ell_n^2}\right] \tag{7}$$

In the above, γ and ϕ are spherical polar angles; relative to unit orthogonal vectors $\vec{a}$, $\vec{b}$ and $\vec{c}$, where $\vec{a}$ is somewhat arbitrarily chosen to lie in the direction of the mean wind velocity and $\vec{c}$ lies in the vertical plane through $\vec{a}$, the angle ϕ is the angle that $\vec{r}$ makes with $\vec{c}$ and γ is the angle between $\vec{a}$ and the projection of $\vec{r}$ on the $\vec{a}$, $\vec{b}$ plane. Thus ℓ_p, ℓ_n, and ℓ_v are respectively the effective scales in the direction of the mean wind, normal to this direction and approximately vertically. It has been found experimentally that the magnitudes of V_n and ℓ_o depend upon the periods of time over which the averages in (5) are taken and the characteristic scale ℓ_o, when determined by averaging over periods of time of the order of an hour, is of the order of hundreds of meters in the troposphere. For this form of correlation function involving scale length ellipsoidal anisotropy, it is shown in Appendix II that the wave-number spectrum of n is given by:

$$S(\vec{k}) = 8\pi\sqrt{\pi}\ \{\Gamma(\mu + \tfrac{3}{2})/\Gamma(\mu)\}\, \ell_p \ell_n \ell_v V_n [1 + (2\pi \ell_k/\ell)^2]^{-\mu - \frac{3}{2}} \tag{8}$$

$$\vec{k} = k(\cos\gamma \sin\phi\ \vec{a} + \sin\gamma \sin\phi\ \vec{b} + \cos\phi\ \vec{c}) \tag{9}$$

$$\ell_k^2 = \ell_p^2 \cos^2\gamma \sin^2\phi + \ell_n^2 \sin^2\gamma \sin^2\phi + \ell_v^2 \cos^2\phi \tag{10}$$

Equation (8) provides a useful model for the spectrum of the turbulence at least for values of $\ell < \ell_k$. If we set $\ell = \lambda/(\alpha + \beta)$ and assume that this is smaller than ℓ_k, then we see by (8) that the wave-number spectrum $S[2\pi(\alpha + \beta)/\lambda, \vec{k}_1]$ associated with the scales appropriate to the forward scatter is proportional to $\ell_p \ell_n \ell_v [\lambda/\ell_k(\alpha + \beta)]^{2\mu + 3}$ and, when this is substituted in (3), we obtain:

$$\Delta L = \Delta L_b = (2\mu + 1)\ 10 \log_{10}(f_2/f_1) \quad [\text{Scaled antennas; } \lambda < (\alpha + \beta)\ell_k] \tag{11}$$

If, as in the Lincoln Laboratory experiment, the antenna gains are not precisely the same and the antenna heights are not scaled, the above becomes:

$$\Delta L_b = (2\mu + 1)\ 10 \log_{10}(f_2/f_1) + H_o(f_2) - H_o(f_1) \tag{12}$$

where the frequency gain function $H_o(2290) = 0$ and $H_o(417) = 0.5$ db in the Lincoln Laboratory experiment. In (11) and (12) we distinguish between the actual transmission loss L and the basic transmission loss $L_b \equiv L + G_p$. It follows from (12) and the data on Fig. 2 that μ exceeds 1.24 for 10% of the hours, exceeds 0.913 for 50% of the hours and exceeds 0.602 for 90% of the hours; note, however, that a 3 db difference in the effects of the terrain on the two frequencies could shift these figures over the ranges indicated on Fig. 2. A shift of

A WAVE NUMBER SPECTRUM $S(\vec{k})$ USEFUL FOR DESCRIBING THE RANDOM VARIATIONS OF THE REFRACTIVE INDEX OVER SPACE

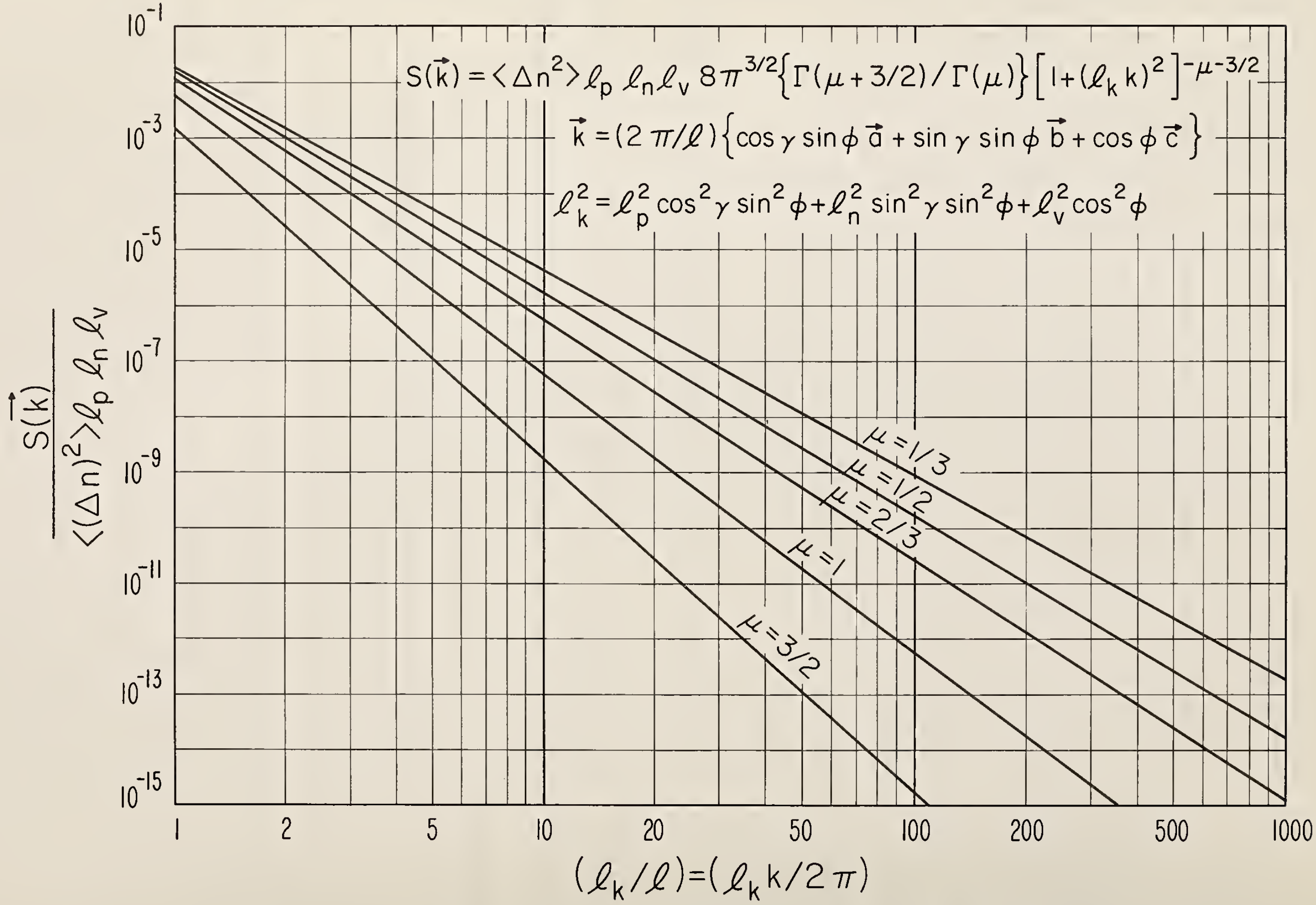

Figure 4

A CORRELATION FUNCTION $C(\vec{r})$ USEFUL FOR DESCRIBING THE RANDOM VARIATIONS OF THE REFRACTIVE INDEX OVER SPACE

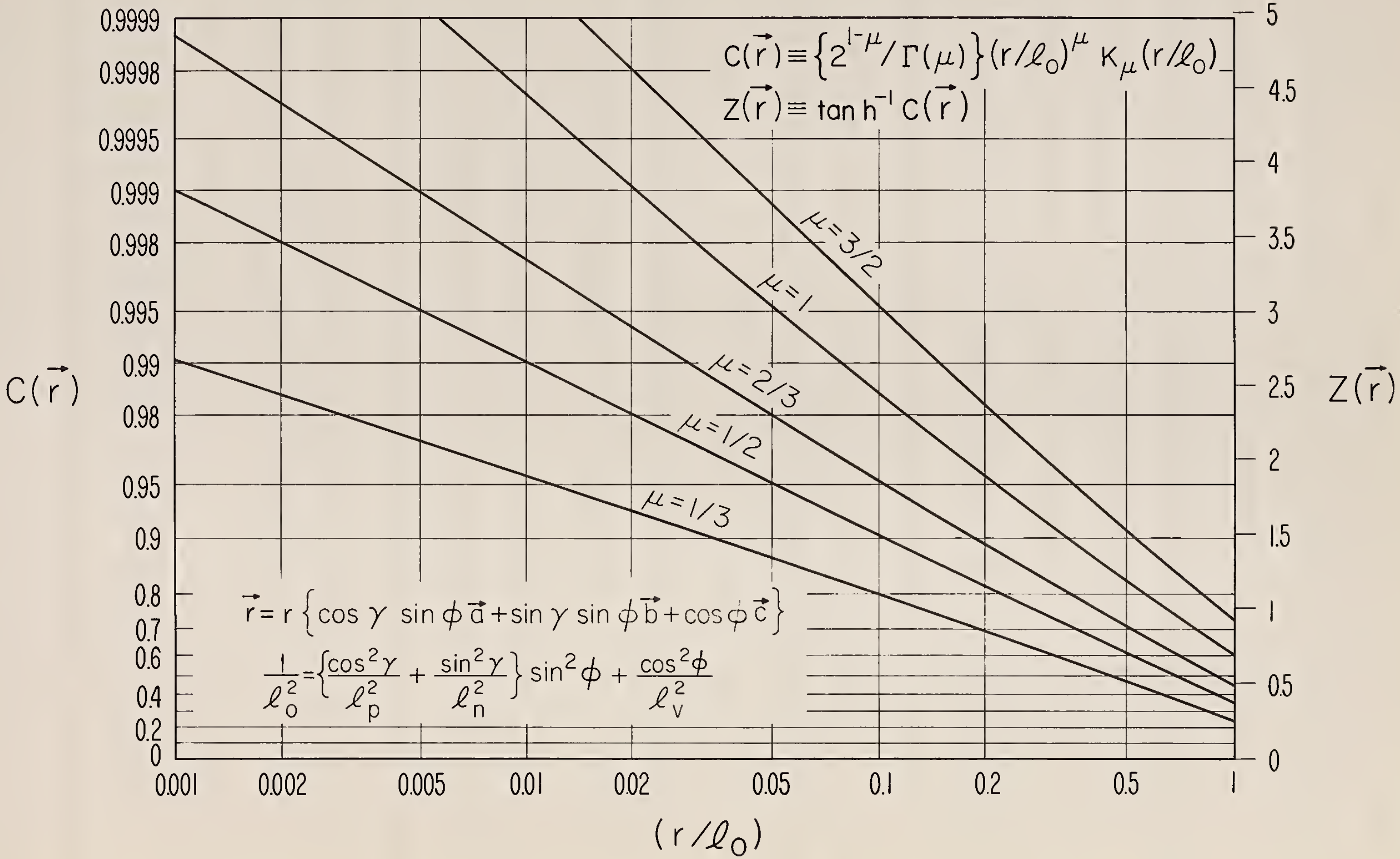

Figure 5

this order of magnitude is not unreasonable to expect in view of the fact that the observed scatter losses on this particular path (See Fig. 1) are systematically several decibels greater than is predicted by the Rice-Longley-Norton formula for average irregular terrain conditions. Fig. 4 shows the wave-number spectrum $S(\vec{k})/\ell_p \ell_n \ell_v V_n$ for several values of μ and, if μ varies from hour to hour, it appears that the slope of $S(\vec{k})$ will vary from hour to hour. Fig. 5 shows $C(\vec{r})$ for several values of μ. On the assumption that n is a normally distributed variable, it is expected that $z(\vec{r}) \equiv \tanh^{-1}\{C(\vec{r})\}$ will also be approximately normally distributed about its true mean value when $C(\vec{r})$ is determined experimentally. 12/ 13/ 15/ For this reason we have also shown $z(\vec{r})$ on a linear scale versus r/ℓ_o on a logarithmic scale on Fig. 5; with these scales the correlation function on Fig. 5 varies linearly for small (r/ℓ_o) with a slope dependent on μ just as its transform S(k) on Fig. 4 varies linearly for large k with its slope also dependent on μ. For $\mu = 0$, $C(\vec{r}) = 1$ for $r = 0$ and $C(\vec{r}) = 0$ for $r > 0$, and such a function is evidently of no interest for describing the atmosphere. A further discussion of the slope of the $z(\vec{r})$ graphs is given in Section 4.

A more precise idea of the influence of μ and of anisotropy on the magnitude of the total scattered power may be obtained by using the particular model (8) for $S(\vec{k})$ and integrating this by the methods given in reference 10. It is assumed that the magnitude of the scattering parameter $\{V_n \ell_p \ell_n / \ell_w \ell_v^{2\mu+1}\}$ has the same value throughout the scattering volume. The transmitting and receiving antennas are assumed to be at the same height above a smooth earth, this height being greater than $4\lambda/\theta$ so that $\bar{g}_t = \bar{g}_r = 2$ for isotropic transmitting and receiving antennas. The antennas are assumed to be a distance d and angular distance θ apart. In this case the median basic scatter transmission loss is expected to be:

$$L_{bms} = -10 \log_{10} < \left[\frac{(\log_e 2)\mu \ \{V_n \ell_p \ell_n / \ell_w\}}{(\mu+1)(2\mu+1)\ d(2\pi \ell_v \theta/\lambda)^{2\mu+1}} \right] > \qquad (13)$$

In the appendix a general formula for L_{bms} is derived for the case where the meteorological scattering parameter $\{V_n \ell_p \ell_n / \ell_w \ell_v^{2\mu+1}\}$ varies inversely as h^m, and the above represents simply the particular case m = 0. For this derivation it is assumed that the mean wind direction lies in the plane which passes through the transmitting and receiving antennas and is normal to the great circle plane; γ is the angle in this plane between the mean wind direction and the great circle plane; using this notation $\ell_w^2 = \ell_p^2 \sin^2\gamma + \ell_n^2 \cos^2\gamma$. When the wind blows along the path, the scattering parameter is $V_n \ell_p / \ell_v^{2\mu+1}$, and when the wind blows across the path, the scattering parameter becomes $V_n \ell_n / \ell_v^{2\mu+1}$. Note the fact that the characteristic scale ℓ_v in the vertical direction enters the scattering parameter with a power 2μ larger than does either ℓ_p or ℓ_n.

We may re-write the general expression (I-8) for the median basic scatter transmission loss in the following form:

$$L_{bms} = -10 \log_{10}\{(\log_e 2)\, V_n \ell_p \ell_n / \ell_w d\}_{h=h_o}$$

$$+ J(\mu, M, S) + (2\mu + 1)\, 10 \log_{10}(2\pi\, \theta \ell_v/\lambda)_{h=h_o} \qquad \text{(I-8a)}$$

If we arbitrarily assume that the first term in (I-8a) does not depend upon μ and does not vary from hour to hour, then we may determine the long-term variance of L_{bms} from the apparent variance of μ shown on Fig. 2, i.e., μ apparently exceeds 0.602 for 90% of the time and apparently exceeds 1.24 for 10% of the time. For the Lincoln Laboratory path $\theta = 0.0271$ and $S = 10 \log_{10}(\beta_o/\alpha_o) = 0.7$, and it is estimated that $M = -4$ db. Since the magnitude of ℓ_v is not known, we will estimate by (I-8a) the interdecile range $L_{bms}(10\%) - L_{bms}(90\%)$ for the two values $\ell_v = 20$ and 200 meters which represent guesses as to the range within which the median value of ℓ_v is expected to lie. The following table gives these calculated values for the two frequencies together with the observed interdecile ranges from Fig. 1.

$L_{bms}(10\%) - L_{bms}(90\%)$

	Observed	Calculated by (I-8a) with ℓ_v = 20 meters	Calculated by (I-8a) with ℓ_v = 200 meters
417 Mc	11.8 db	8.6 db	21.4 db
2290 Mc	10.5 db	18.0 db	30.8 db

It is evident from the above table that the observed interdecile ranges do not agree with those calculated on the assumption that the variations of μ are responsible for all of the variance of L_{bms}; in particular, the observed variance is slightly smaller on the higher frequency, and this is inconsistent with the assumption that <u>any</u> of the variance arises from variations in μ. Furthermore, if the variance of L_{bms} is attributed to a variance of μ, then we see by (I-8a) that the long-term variance of L_{bms} would be expected to increase systematically with the angular distance θ; for the winter afternoon hours when scatter would be expected, the observed variance of L_{bms} appears to decrease with θ rather than increasing with θ. This analysis indicates to the author that μ probably varies, if at all, over a much smaller range than is indicated on Fig. 2, and that the variance of L_{bms} from hour to hour must be attributed to a variance in the first term of (I-8a) together with a variance of ℓ_v rather than to a variance of μ.

Further evidence as to the nature of the hour-to-hour variance of L_b is given on Fig. 6. This shows the observed hourly median scatter values of L_b for both 417 Mc and 2290 Mc as a function of ΔL_b. If a variance of μ were responsible for all of the variance of L_b, then L_b would be expected on both frequencies to increase linearly with ΔL_b with a larger slope on the higher frequency; instead L_b has

SCATTER LOSSES FROM THE LINCOLN LABORATORY EXPERIMENT

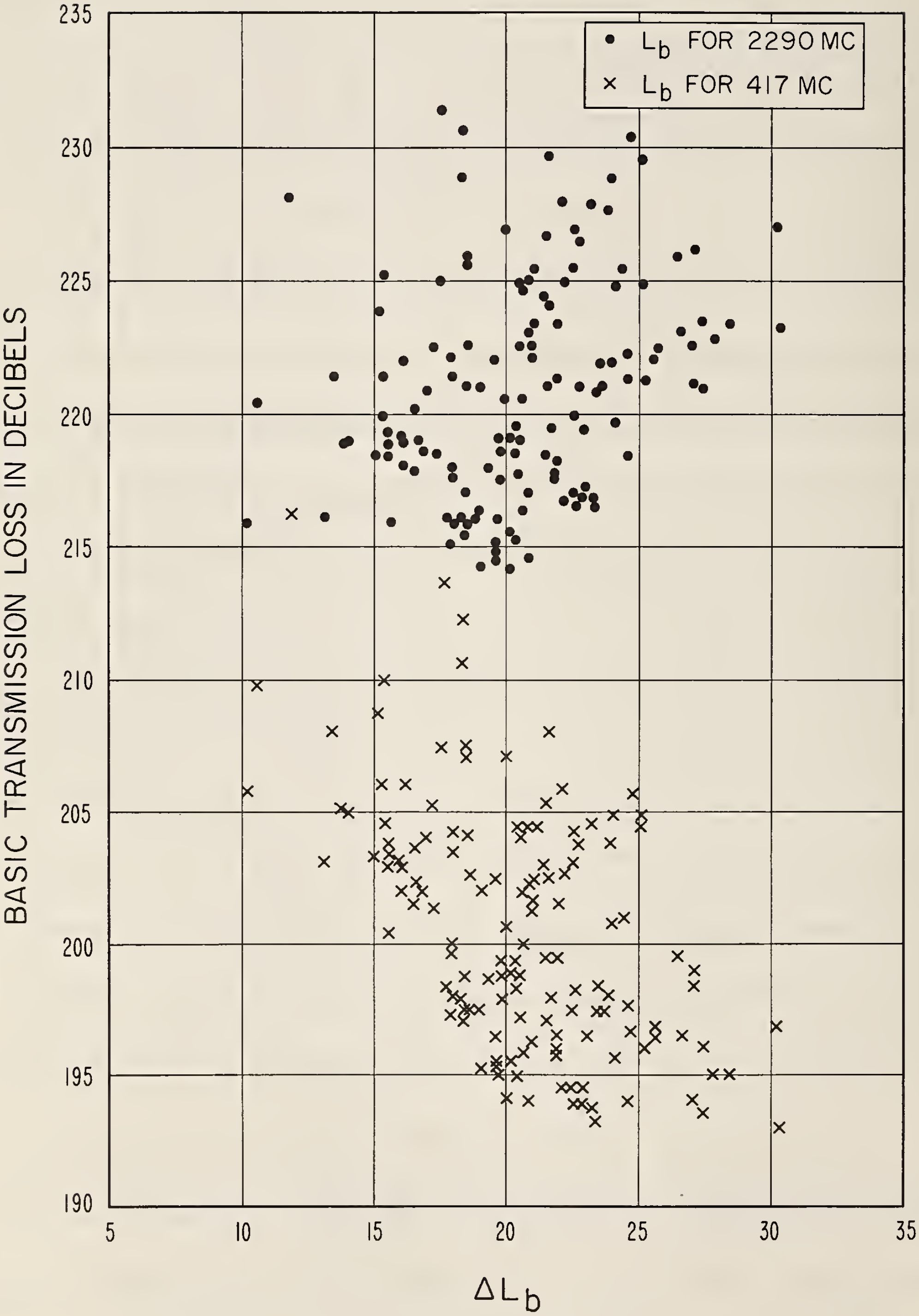

Figure 6

little or no dependence on ΔL_b, although it appears actually to decrease with increasing ΔL_b on 417 Mc.

4. Meteorological Measurements Useful for Evaluating L_{bms}

In this section we will consider how meteorological measurements might be made in order to evaluate the magnitude of the scattering parameter $\{V_n \ell_p \ell_n / \ell_w \ell_v^{2\mu + 1}\}$. Since direct measurements of $S(\vec{k})$ cannot be made, it appears to be almost essential, particularly if the variations of n are anisotropic, to measure $C(\vec{r})$ for several values of the magnitude and direction of $\vec{r}$, use these measurements to develop an appropriate model for $C(\vec{r})$ and finally determine $S(\vec{k})$ as the cosine-space transform (4) of this model $C(\vec{r})$.

The following experiment using a minimum of five refractometers mounted on a tethered balloon or aircraft is suggested. Three of the refractometers should be located on a vertical line with locations $r = 0$, r_1, and $3r_1$ and the other two located on a horizontal line normal to the direction of flight and with spacings relative to one of the three vertically spaced refractometers equal to r_1 and $3r_1$. In this way it will be possible to measure $C(\vec{r})$ corresponding to spacings r_1, $3r_1 - r_1 = 2r_1$, and $3r_1$. By plotting the resulting six values of $C(\vec{r})$ on graph paper similar to that of Fig. 5 and shifting this to the right or left until the points best fit one of the curves of Fig. 5, estimates can be obtained of μ and ℓ_o. If these estimates indicate significantly different values of either μ or ℓ_o or both for three points obtained from the vertically and horizontally spaced refractometers, then it would appear that the variations of n are anisotropic. If μ is a function of the direction of $\vec{r}$, then we must abandon our model function (8). If μ is independent of the direction of $\vec{r}$ but ℓ_o is variable, then the measured value of ℓ_o along the vertical line may be identified with ℓ_v and the measured value of ℓ_o along the horizontal line may be identified with ℓ_n when the plane flies with or against the wind, and may be identified with ℓ_p when the plane flies normal to the direction of the wind. Assuming that the measurements are designed to test the forward scatter theory for a path with angular distance θ and on a frequency corresponding to a free space wavelength λ, it will be desirable to choose $3r_1 = \lambda/\theta$ and then fly the aircraft throughout that part of the common volume most intensely illuminated by both the transmitting and receiving antennas. Note that five independent measurements of V_n will be available and these may be averaged. In order to represent hourly median scattered fields the balloon measurements should be averaged over an hour, but the aircraft measurements could be averaged over a shorter period in the ratio of the mean wind speed to air speed.

If the variations of n are found experimentally to be isotropic for the small scales $\lambda/3\theta$, $\lambda/(3/2)\theta$ and λ/θ involved in such an experiment, then we may estimate $S(2\pi/\ell)$, which will now be independent of the direction $\vec{k}_1$, as follows:

$$S(k) \cong \frac{\mu\,\Gamma(\mu + \frac{3}{2})}{2\pi^{2\mu + \frac{3}{2}}\,\Gamma(1 - \mu)} \cdot \ell^3 <[\delta n(\ell)]^2> \tag{14}$$

Here $\delta n(\ell, \vec{r}_1) \equiv n(\vec{R}) - n(\vec{R} + \ell\,\vec{r}_1)$ and $<[\delta n(\ell)]^2>$ is the structure function for the turbulence; since we are here assuming the turbulence to be isotropic, the expected value of $<[\delta n(\ell)]^2>$ will be independent of the direction of $\vec{r}_1$ and equal to:

$$<[\delta n(\ell)]^2> = 2\,V_n[1 - C(\ell)] \tag{15}$$

For small values of $\ell << \ell_o$, $C(\ell) = 1 - \{\Gamma(1-\mu)/\Gamma(1+\mu)\}(\ell/2\ell_o)^{2\mu}$ for $\mu < 1$, provided the correlation function has the form (6) and, when this value is introduced into (15) we obtain $<[\delta n(\ell)]^2> = 2\,V_n\{\Gamma(1-\mu)/\Gamma(1+\mu)\}(\ell/2\ell_o)^{2\mu}$; when this value is in turn substituted in (14), it becomes equal to (8) for the special case of isotropic n variations. Note now that the structure function $<[\delta n(\ell)]^2>$ can be measured directly in the above-described experiment with refractometers. If the ratios $<[\delta n(r_1)]^2>/<[\delta n(2\,r_1)]^2>/<[\delta n(3r_1)]^2>$ obtained by averaging over a period of an hour are the same from hour to hour, then it appears that μ is also constant and we must look elsewhere for the explanation of the observed variations shown on Fig. 2.

Finally it will be useful to consider the nature of the correlation function (6) as shown graphically on Fig. 5. The slope D of those curves is given by:

$$D = \frac{\partial z}{\partial[\ln(r/\ell_o)]} = \frac{1}{1 - [C(r/\ell_o)]^2} \cdot \frac{\partial[C(r/\ell_o)]}{\partial[\ln(r/\ell_o)]} \tag{16}$$

We will be interested in D for $r << \ell_o$ and we may set $C(r/\ell_o) = 1 - \Delta C(r/\ell_o)$ where $\Delta C(r/\ell_o) << 1$; thus:

$$D \cong \frac{-\partial[\Delta C(r/\ell_o)]}{2\Delta C(r/\ell_o)\,\partial[\ln(r/\ell_o)]} = \frac{-\partial\{\ln[\Delta C(r/\ell_o)]\}}{2\partial[\ln(r/\ell_o)]} \tag{17}$$

For $\mu < 1$ and $r << \ell_o$, $\Delta C(r/\ell_o) = \{\Gamma(1-\mu)/\Gamma(1+\mu)\}(r/2\ell_o)^{2\mu}$ and thus:

$$D \cong -\mu \qquad \text{For } 0 < \mu < 1 \text{ and } r << \ell_o \tag{18}$$

The above is illustrated on Fig. 5; for $\mu \geq 1$ it can be shown that D approaches -1 as r approaches zero; however, within the scale ranges shown on Fig. 5, the slope D continues to increase with increasing μ between $\mu = 1$ and $\mu = 1.5$, and we may still use this slope as a means for determining μ.

It should be noted that single refractometers have been used to investigate the <u>frequency</u> spectrum 14/ 15/ 16/ 18/ of refractivity and the correlation with <u>time</u> of the refractivity at a single location in the atmosphere, but the wave-number spectrum $S(\vec{k})$ and the correlation function $C(\vec{r})$ may be inferred from such results only on the assumption (essentially Taylor's hypothesis) that all of the variation of n occurs as a result of the drift of a frozen atmospheric pattern through the refractometer without any significant change in this pattern due to the self-motion of the atmosphere during the time occupied by the measurements. As Gifford [19] has pointed out, the connection between the space-and time-turbulence statistics cannot be said to be well understood in the case of the free atmosphere as contrasted to the wind tunnel. Gossard [18] claims to have verified Taylor's hypothesis by approximating a measurement of the wave-number spectrum by flying rapidly through the atmosphere with a refractometer on an aircraft and then comparing these results with those obtained indirectly from the frequency spectrum of refractivity measured with a refractometer on a tethered balloon; however, his aircraft spectra are definitely steeper (larger μ) than the indirectly determined balloon spectra at the higher wave numbers, and thus I would interpret his results as being in disagreement with Taylor's hypothesis.

Aside from the above difficulty arising from a possible failure of Taylor's hypothesis, an even more important difficulty with the spectra determined with single refractometers is the fact that they measure only the variations of refractivity in the horizontal direction, and we have seen above that it is the refractivity in the vertical direction that is more important as regards the forward scatter of radio waves.

For the above reasons it appears most desirable that the above-described direct measurements of $C(\vec{r})$ be made using several refractometers simultaneously with appropriately chosen spacings along a vertical line and, in the horizontal plane, along two lines parallel and normal to the average wind velocity.

Acknowledgements: The author wishes to acknowledge the assistance in the development of this paper which was obtained in several stimulating discussions with his colleagues E. C. Barrows, P.L. Rice, W. J. Hartman and R. L. Abbott, as well as with Prof. Ralph Bolgiano of Cornell University. William V. Mansfield supplied the values in Table III. Jack C. Stroud assisted with some of the statistical calculations. Mrs. A. G. Longley carried out the analysis in Appendix III.

Appendix I

Derivation of a General Formula for the Median Basic Scatter Transmission Loss

The median basic scatter transmission loss may be expressed [4] [15] as follows:

$$L_{bms} = -10 \log_{10}\left[\frac{(\log_e 2)\langle p_s\rangle}{p_t}\right] = -10 \log_{10}\left[\frac{\log_e 2}{4k_f^2}\int \frac{g_t\, g_r \langle\sigma\rangle\, dv}{(R\, R_o)^2}\right] \tag{I-1}$$

The time averages $\langle\ \rangle$ are to be taken over the short period of time for which the median is specified and this period of time must be sufficiently short (only a few minutes at 1000 Mc) so that the distribution of p_s within that period may be represented by the Rayleigh distribution. In the above, $k_f = 2\pi/\lambda$ where λ is the wavelength in free space and the integration is taken over the common volume. Fig. 7 illustrates the geometry involved in the evaluation of the scattering integral and certain approximations made in this evaluation; the justification for these approximations is given in reference 15 and later in this appendix. The following derivation is given for the case where the transmitting and receiving antennas are at the same height over a smooth earth and sufficiently high ($h_{te} = h_{re} > 4\lambda/\theta$) above the ground so that the sine-squared oscillations of g_t and g_r occur within sufficiently small intervals

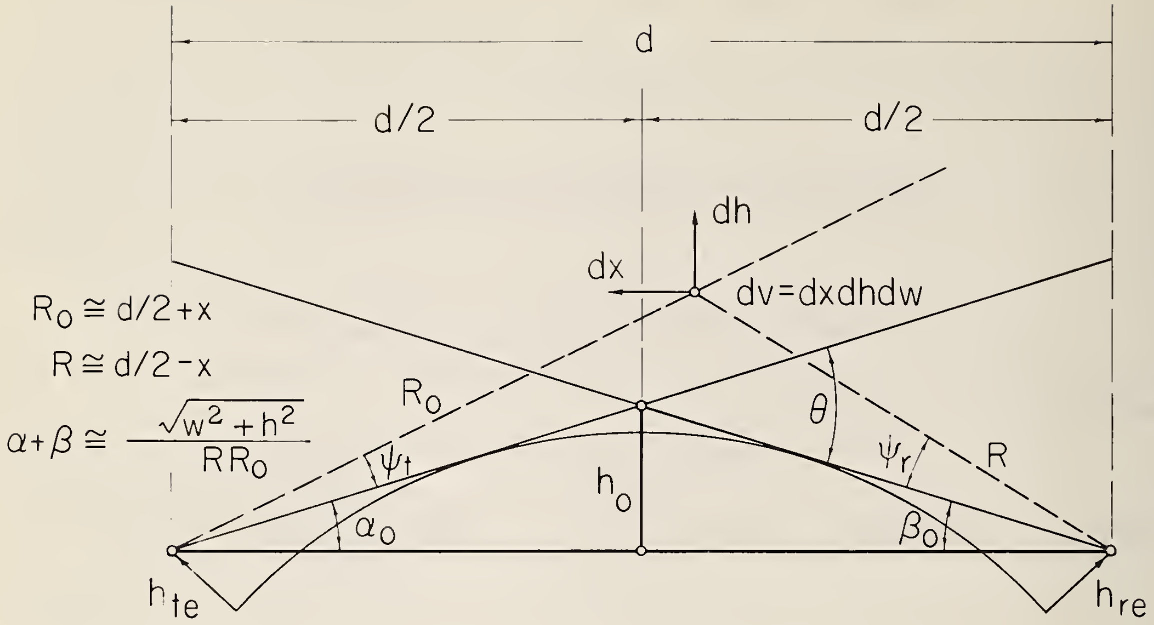

PLAN VIEW

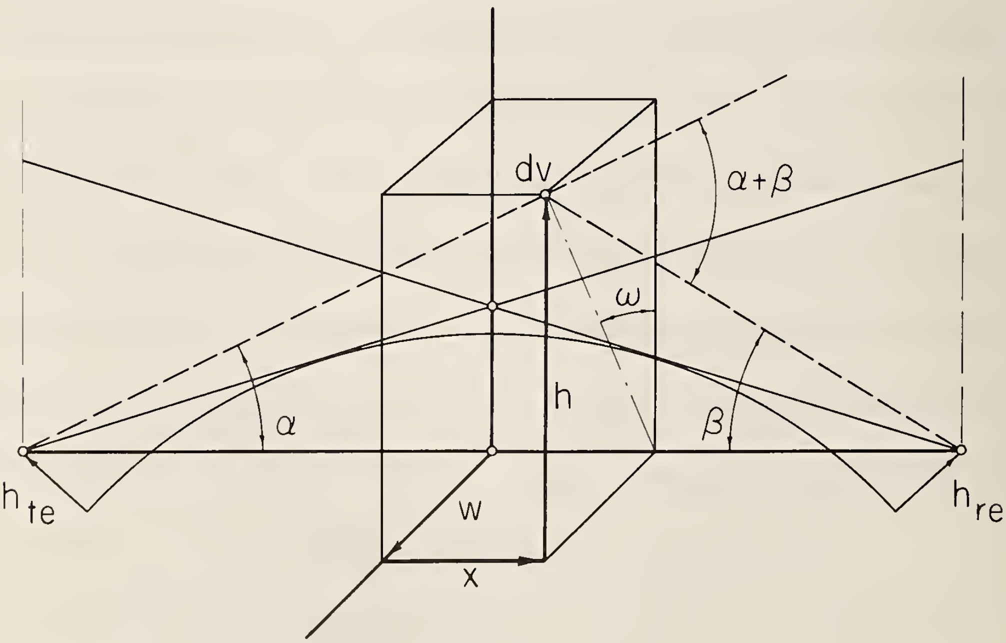

Figure 7

of ψ_t and ψ_r so that the product $\overline{g}_t \overline{g}_r = 4$ and the frequency gain function is equal to zero.

We will evaluate (I-1) for an atmosphere characterized by the correlation function (6) and corresponding to the wave-number spectrum (8) for which the average scattering cross section $< \sigma >$ may be expressed: 8/ 10/

$$< \sigma > \cong \{2 k_f^4 \sin^2 \chi / \sqrt{\pi}\} < \{\Gamma(\mu + \tfrac{3}{2}) / \Gamma(\mu)\} V_n \ell_p \ell_n \ell_v q^{-2\mu - 3} > \quad \text{(I-2)}$$

$$q \cong k_f(\alpha + \beta) \{[\ell_p^2 \sin^2 \gamma + \ell_n^2 \cos^2 \gamma] \sin^2 \omega + \ell_v^2 \cos^2 \omega\}^{1/2} \quad \text{(I-3)}$$

The approximation in (I-2) is negligible for $q > 2\pi$. See reference 10 for the derivation of (I-3); the small approximation involved in the derivation of (I-3) is equivalent to the assumption that the vector $\vec{k}_1$ lies in planes perpendicular to the line joining the antennas. In the above we have assumed that the mean wind direction lies in the plane which passes through the transmitting and receiving antennas and is normal to the great circle plane; and γ is the angle in this plane between the mean wind direction and the great circle plane; $\sin \omega \equiv w(w^2 + h^2)^{-1/2}$. Now make the following substitution:

$$\ell_p^2 \sin^2 \gamma + \ell_n^2 \cos^2 \gamma \equiv \ell_w^2 \quad \text{(I-4)}$$

$$\alpha + \beta \cong d(w^2 + h^2)^{1/2} / R R_o \quad \text{(I-5)}$$

$$q \cong (k_f d / R R_o) \{(w \ell_w)^2 + (h \ell_v)^2\}^{1/2} \quad \text{(I-6)}$$

For the following evaluation we will set $\sin^2 \chi = 1$ and will assume that the meteorological parameter $\{V_n \ell_p \ell_n / \ell_w \ell_v^{2\mu+1}\} \sim (h_o/h)^m$ where h_o is the height of the cross-over of the radio horizon rays; now (I-1) becomes:

$$L_{bms} \cong -10 \log_{10} < \left[\frac{4(\log_e 2)\Gamma(\mu+\frac{3}{2})\{V_n \ell_p \ell_n \ell_v\}_{h=h_o} h_o^m}{\sqrt{\pi}\,\Gamma(\mu)\, k_f^{2\mu+1} d^{2\mu+3}} \int_o^{\frac{d}{2}} \left[\left(\frac{d}{2} - x\right)\left(\frac{d}{2} + x\right)\right]^{2\mu+1} dx \int_{\beta_o(\frac{d}{2}+x)}^{\infty} \frac{dh}{h^m} \int_{-\infty}^{+\infty} \frac{dw}{\{(w\ell_w)^2 + (h\ell_v)^2\}^{(2\mu+3)/2}} \right] > \tag{I-7}$$

The integral with respect to w is readily evaluated by a change of variable $z = w\ell_w / h\ell_v$:

$$\int_{-\infty}^{+\infty} \frac{dw}{\{(w\ell_w)^2 + (h\ell_v)^2\}^{(2\mu+3)/2}} = \frac{1}{\ell_w (h\ell_v)^{2\mu+2}} \int_{-\infty}^{+\infty} \frac{dz}{\{1 + z^2\}^{(2\mu+3)/2}} = \frac{\Gamma(\frac{1}{2})\,\Gamma(\mu+1)}{\ell_w (h\ell_v)^{2\mu+2}\,\Gamma(\mu+\frac{3}{2})}$$

The integration with respect to h may now be performed and we obtain finally:

$$L_{bms} \cong -10 \log_{10} < \left[\frac{(\log_e 2)\{V_n \ell_p \ell_n / \ell_w\}_{h=h_o} I(\mu, m)}{d(2\pi\,\theta\ell_v/\lambda)^{2\mu+1}_{h=h_o}} \right] > \tag{I-8}$$

where the numerical constant

$$I(\mu, m) \equiv \frac{2\mu}{(2\mu+1+m)} \int_o^1 \frac{x^{2\mu+1}\,dx}{(2-x)^m} \tag{I-9}$$

The only restrictions on the validity of (I-8) are that $\theta << 1$ and $\lambda << \theta\ell_o$.

For an average atmosphere ($N_s = 316$), the effective radius of the earth a = 9000 km and the distance between the antennas, d_g, along the ground in the great circle plane is given by:

$$d_g\,(\text{km}) \cong a\,\theta + 3\sqrt{2h_{te}\,(\text{meters})} + 3\sqrt{2h_{re}\,(\text{meters})} \qquad \text{(I-10)}$$

The expression $3\sqrt{2h_{te}\,(\text{meters})}$ in (I-10) for the distance, d_h, to the radio horizon from a height h_{te} is quite accurate for those antenna heights likely to be involved in tropospheric scatter systems, and may be corrected for the higher heights in the exponential atmosphere corresponding to $N_s = 316$ by the method of Bean and Thayer; [11] thus $d_h\,(\text{km}) = 3\sqrt{2h_{te}\,(\text{meters})} - \Delta d$ where $\Delta d = 0.25$ km for $h_{te} = 500$ meters, $\Delta d = 1.82$ km for $h_{te} = 2$ km, $\Delta d = 6.44$ km for $h_{te} = 5$ km and $\Delta d = 15.39$ km for $h_{te} = 10$ km. The distance d in (I-8) may now be determined from:

$$d = 2(a + h_{te})\sin[d_g/2a] \cong d_g \qquad \text{(I-11)}$$

In order to show that the geometrical approximations made in the integrations leading to (I-8) are negligible, we will obtain the same solution by a different method for the special case $\mu = 0.5$, $m = 0$, and $\lambda << \theta\ell_o$ assuming isotropic turbulence $\ell_p = \ell_n = \ell_v = \ell_o$. The method of integration is the same as that employed in an early paper by Herbstreit, Norton, Rice, and Schafer. [17] We will set $\sin^2\chi = 1$ and $\bar{g}_t\,\bar{g}_r = 4$ as before, $dv = d\alpha\, d\beta\, d\omega (R\,R_o)^2/d$ and then we obtain for the special case $\mu = 0.5$ and $m = 0$:

$$L_{bms} = -10\log_{10}\left[\frac{1}{4\pi d k_f^2}\int_{-\frac{\pi}{2}}^{+\frac{\pi}{2}} d\omega \int_{\beta_m}^{\pi-\alpha_m} d\beta \int_{\alpha_m}^{\pi-\beta} \frac{\{V_n/\ell_o\}\,d\alpha}{\{\sin(\frac{\alpha+\beta}{2})\}^4}\right] \tag{I-11}$$

If now we replace the spherical earth by a cylinder with its axis perpendicular to the great circle plane (a very good approximation), the lower limits α_m and β_m may be expressed:

$$\alpha_m = \tan^{-1}(\tan\alpha_o/\cos\omega) \tag{I-12}$$

$$\beta_m = \tan^{-1}(\tan\beta_o/\cos\omega) \tag{I-13}$$

All of the integrations in (I-11) may now be performed for our particular case$(\alpha_o = \beta_o)$and we obtain:

$$L_{bms} = -10\log_{10}\left[\frac{(\log_e 2)\,V_n\ell_o}{6d(2\pi\ell_o\theta/\lambda)^2}\left\{\frac{\alpha_o^2}{\tan^2\alpha_o} + 8\alpha_o^2\,\ell n\left(\frac{1+\sin\alpha_o}{2\sin\alpha_o}\right)\right\}\right] \tag{I-14}$$

The above may be written:

$$L_{bms} = L_{bms}(\theta << 1) - \Delta L(\theta) \tag{I-15}$$

where $L_{bms}(\theta << 1)$ is identical to (13) for $\mu = \frac{1}{2}$ and $m = 0$ and:

$$\Delta L(\theta) = 10\log_{10}\left\{\frac{\alpha_o^2}{\tan^2\alpha_o} + 8\alpha_o^2\,\ell n\left(\frac{1+\sin\alpha_o}{2\sin\alpha_o}\right)\right\} \tag{I-16}$$

$\Delta L(\theta) = 0.193$ db for $\theta = 0.1$, $\Delta L(\theta) = 0.354$ db for $\theta = 0.15$ and $\Delta L(\theta) = 0.530$ db for $\theta = 0.2$; since this small correction term will be even smaller for $m > 0$, it may be considered negligible for practical applications since m will be large whenever θ is large.

It appears from the above discussion that the comparatively simple formula (I-8) will yield precise results in most practical applications. In practice it will be found that the meteorological parameter will not vary as $(h_o/h)^m$ except over small ranges of h. However, we may still use (I-8) with quite good accuracy for the more general case in which the height dependence is given by:

$$(V_n \ell_p \ell_n / \ell_w \ell_v^{2\mu + 1})_{h = h_o} f(h) \tag{I-17}$$

where $f(h_o) = 1$ simply by setting $f'(h_o) = \left[\frac{d}{dh} \left(\frac{h_o}{h} \right)^m \right]_{h = h_o}$ and solving for m:

$$m = - h_o f'(h_o) \tag{I-18}$$

For example, there are good reasons to believe that the meteorological parameter varies approximately exponentially with the height, at least for large heights, in which case $f(h) = \exp[-(h - h_o)/H(h_o)]$ where $H(h_o)$ is a scale height which is a very slowly varying function of h_o; the appropriate value of m to use in (I-8) to approximate this exponential variation is thus $m = h_o/H(h_o)$.

Unfortunately the above approximate method of allowing for some functional dependence of the meteorological parameter other than $(h_o/h)^m$ will not provide accurate results in many important cases. For example, a solution for the basic scatter transmission loss has been obtained by Rice, Longley and Norton [5/] for the case $\mu = 1$ using an exponential function of h, and the following table gives the difference in decibels between this exact solution and the approximate solution using (I-8) with $m = h_o/H(h_o)$.

Table II

m	d_g (km)	θ	$L_{bms}(RLN) - L_{bms}(I\text{-}8)$	C
0.001	88	0.00031	0.005	2.70
0.01	108	0.0027	0.087	3.05
0.1	208	0.0135	0.829	2.91
1	530	0.052	6.717	2.55
10	1470	0.181	48.86	2.12

The distance d_g and angular distance θ in Table II were calculated for the case $h_{te} = h_{re} = 100$ meters and for the particular Bean and Thayer [11/] exponential atmosphere corresponding to $N_s = 316.29$; this atmosphere corresponds, with an actual earth's radius of 6370 km, to an effective earth's radius of 9000 km. For this atmosphere $H(h_o) = 6.8925$ km for all values of h_o. We see by Table II that the approximate formula (I-8) seriously underestimates the basic scatter transmission loss when d_g is very large. This error can be eliminated by equating the derivatives at some larger height $h_c = C h_o$, i.e., by setting $m = C h_o/H(C h_o)$, and the required values of C are given in Table II; however, since the proper value of C to use in any given instance depends upon the function f(h) assumed, this method of eliminating the errors in (I-8) for functions f(h) other than $(h_o/h)^m$ is impracticable.

The formula (I-8) may be readily extended to the case of an unsymmetrical path (see references 4 or 15 for the geometry) such as is usually encountered over irregular terrain or over smooth terrain with unequal antenna heights. For this case the only change in the above theory is in the term $I(\mu, m)$ which now depends on the additional parameter $s \equiv (\alpha_o/\beta_o)$:

$$I(\mu, m, s) \equiv \frac{2\mu}{(s+1)(2\mu+1+m)} \left\{ s^m \int_o^1 \frac{x^{2\mu+1}\,dx}{(s+1-x)^m} + s^{1-m} \int_o^1 \frac{x^{2\mu+1}\,dx}{(\frac{1}{s}+1-x)^m} \right\} \tag{I-19}$$

For the numerical evaluation of (I-8) it is convenient to tabulate the value of $I(\mu, m, s)$ in the form:

$$J(\mu, M, S) \equiv -10 \log_{10} I(\mu, m, s) \tag{I-20}$$

as a function of the parameters μ, $S \equiv 10 \log_{10} s$ and $M \equiv 10 \log_{10} m$; such a tabulation is given in Table III. Note that $I(\mu, m, 1/s) = I(\mu, m, s)$ and thus the same value $J(\mu, M, S)$ may be tabulated for $\pm S$. The values in Table III were obtained by numerical integration using an IBM 650 computer; the tabulated values are correct to the nearest 0.001 db, and it should be possible to interpolate linearly in this table with an accuracy better than 0.05 db for any intermediate values of μ, M and S. When 2μ is an integer, $I(\mu, m, s)$ may be evaluated in closed form as may be seen from the following expression:

$$I(\mu, m, s) \equiv \frac{2\mu}{(s+1)(2\mu+1+m)} \left\{ s^m \int_s^{1+s} \frac{(s+1-x)^{2\mu+1} dx}{x^m} + s^{1-m} \int_{1/s}^{1+1/s} \frac{(\frac{1}{s}+1-x)^{2\mu+1} dx}{x^m} \right\}$$

The above expression was used for $\mu = 1$ as a check on the accuracy of a few of the values obtained by numerical integration.

Table III

$J(\mu, M, 0)$

M	$\mu =$ 0.32	$\mu =$ 0.34	$\mu =$ 0.36	$\mu =$ 0.38	$\mu =$ 0.40	$\mu =$ 0.45	$\mu =$ 0.50	$\mu =$ 0.55	$\mu =$ 0.60	$\mu =$ 0.70	$\mu =$ 0.80	$\mu =$ 1.0	$\mu =$ 1.2	$\mu =$ 1.5
$-\infty$	8.303	8.209	8.128	8.056	7.993	7.869	7.782	7.722	7.677	7.656	7.672	7.782	7.947	8.239
-30	8.306	8.213	8.131	8.060	7.997	7.872	7.785	7.725	7.687	7.658	7.674	7.784	7.949	8.241
-25	8.314	8.221	8.139	8.067	8.004	7.879	7.791	7.731	7.693	7.664	7.679	7.788	7.953	8.245
-20	8.339	8.245	8.163	8.090	8.027	7.901	7.812	7.752	7.712	7.682	7.696	7.804	7.967	8.256
-18	8.360	8.266	8.183	8.110	8.047	7.920	7.830	7.769	7.729	7.698	7.711	7.816	7.979	8.266
-16	8.394	8.299	8.215	8.142	8.078	7.950	7.859	7.796	7.755	7.722	7.734	7.837	7.997	8.282
-14	8.447	8.350	8.266	8.192	8.127	7.997	7.904	7.839	7.797	7.761	7.770	7.869	8.026	8.308
-12	8.530	8.432	8.346	8.270	8.204	8.070	7.974	7.907	7.862	7.821	7.827	7.919	8.071	8.347
-10	8.659	8.559	8.471	8.393	8.324	8.185	8.085	8.013	7.965	7.917	7.916	7.999	8.143	8.410
-9	8.749	8.647	8.557	8.478	8.407	8.265	8.162	8.087	8.036	7.983	7.979	8.054	8.193	8.454
-8	8.860	8.757	8.665	8.583	8.511	8.365	8.257	8.179	8.125	8.066	8.056	8.124	8.256	8.509
-7	8.999	8.892	8.798	8.714	8.640	8.489	8.376	8.294	8.235	8.169	8.153	8.210	8.334	8.577
-6	9.169	9.060	8.963	8.876	8.799	8.642	8.523	8.436	8.372	8.298	8.274	8.318	8.432	8.663
-5	9.379	9.266	9.166	9.076	8.996	8.830	8.705	8.611	8.541	8.456	8.423	8.452	8.553	8.769
-4	9.636	9.519	9.414	9.320	9.236	9.062	8.929	8.827	8.750	8.652	8.608	8.617	8.703	8.902
-3	9.949	9.826	9.717	9.619	9.530	9.345	9.202	9.091	9.006	8.892	8.834	8.822	8.889	9.066
-2	10.326	10.198	10.083	9.980	9.886	9.689	9.534	9.413	9.317	9.186	9.112	9.072	9.118	9.268
-1	10.779	10.645	10.524	10.414	10.314	10.103	9.935	9.802	9.695	9.543	9.450	9.379	9.398	9.517
0	11.318	11.177	11.049	10.932	10.826	10.599	10.416	10.268	10.149	9.973	9.858	9.750	9.739	9.821
1	11.954	11.805	11.669	11.544	11.431	11.186	10.987	10.824	10.690	10.487	10.348	10.198	10.152	10.190
2	12.696	12.538	12.394	12.262	12.140	11.877	11.660	11.480	11.329	11.096	10.931	10.733	10.647	10.635
3	13.555	13.388	13.235	13.094	12.964	12.680	12.444	12.245	12.077	11.811	11.616	11.366	11.235	11.168
4	14.537	14.361	14.198	14.048	13.910	13.604	13.348	13.130	12.943	12.642	12.415	12.108	11.928	11.799
5	15.648	15.462	15.290	15.131	14.983	14.656	14.378	14.140	13.934	13.597	13.335	12.968	12.735	12.539
6	16.889	16.693	16.512	16.344	16.187	15.837	15.538	15.279	15.053	14.679	14.383	13.952	13.664	13.395
7	18.258	18.053	17.862	17.685	17.518	17.147	16.826	16.547	16.301	15.889	15.558	15.064	14.719	14.375
8	19.747	19.532	19.333	19.146	18.972	18.579	18.238	17.939	17.674	17.225	16.860	16.302	15.900	15.481
9	21.342	21.119	20.912	20.717	20.534	20.122	19.762	19.444	19.161	18.678	18.280	17.661	17.204	16.711
10	23.028	22.798	22.582	22.381	22.191	21.760	21.383	21.049	20.749	20.235	19.806	19.131	18.622	18.059
11	24.786	24.549	24.328	24.120	23.924	23.478	23.086	22.737	22.423	21.881	21.425	20.700	20.144	19.515
12	26.600	26.358	26.132	25.918	25.717	25.259	24.854	24.492	24.166	23.600	23.122	22.352	21.754	21.068
13	28.457	28.211	27.980	27.762	27.557	27.088	26.673	26.301	25.965	25.379	24.881	24.074	23.441	22.704

Table III

J (μ, M, ±2)

M	μ = 0.32	μ = 0.34	μ = 0.36	μ = 0.38	μ = 0.40	μ = 0.45	μ = 0.50	μ = 0.55	μ = 0.60	μ = 0.70	μ = 0.80	μ = 1.0	μ = 1.2	μ = 1.5
-∞	8.303	8.209	8.128	8.056	7.993	7.869	7.782	7.722	7.677	7.656	7.672	7.782	7.947	8.239
-30	8.306	8.213	8.131	8.060	7.997	7.872	7.785	7.725	7.687	7.658	7.674	7.784	7.949	8.241
-25	8.315	8.221	8.139	8.067	8.005	7.880	7.792	7.732	7.693	7.664	7.680	7.789	7.954	8.245
-20	8.341	8.247	8.164	8.092	8.029	7.903	7.814	7.753	7.714	7.683	7.698	7.805	7.968	8.257
-18	8.363	8.268	8.185	8.113	8.049	7.922	7.833	7.771	7.731	7.700	7.713	7.818	7.980	8.268
-16	8.398	8.303	8.219	8.146	8.082	7.953	7.862	7.800	7.759	7.725	7.737	7.840	8.000	8.285
-14	8.453	8.356	8.272	8.198	8.133	8.002	7.909	7.845	7.802	7.766	7.775	7.874	8.030	8.312
-12	8.539	8.441	8.355	8.280	8.213	8.079	7.983	7.916	7.871	7.830	7.835	7.927	8.079	8.354
-10	8.674	8.574	8.486	8.408	8.339	8.200	8.099	8.027	7.978	7.930	7.929	8.011	8.155	8.421
-9	8.768	8.666	8.576	8.496	8.426	8.284	8.180	8.105	8.053	8.000	7.995	8.070	8.208	8.467
-8	8.884	8.780	8.688	8.606	8.534	8.388	8.280	8.201	8.146	8.087	8.077	8.143	8.274	8.525
-7	9.028	8.922	8.827	8.743	8.669	8.517	8.404	8.321	8.262	8.196	8.179	8.234	8.357	8.598
-6	9.206	9.096	8.999	8.912	8.835	8.677	8.558	8.470	8.405	8.330	8.305	8.348	8.460	8.689
-5	9.425	9.312	9.211	9.121	9.040	8.874	8.748	8.653	8.583	8.497	8.462	8.489	8.588	8.802
-4	9.692	9.575	9.470	9.376	9.291	9.116	8.982	8.879	8.801	8.702	8.656	8.663	8.747	8.942
-3	10.018	9.895	9.785	9.686	9.597	9.411	9.267	9.155	9.069	8.954	8.894	8.878	8.943	9.115
-2	10.410	10.282	10.166	10.062	9.968	9.769	9.614	9.491	9.394	9.261	9.185	9.141	9.184	9.329
-1	10.881	10.746	10.624	10.514	10.413	10.201	10.032	9.896	9.788	9.634	9.539	9.462	9.478	9.591
0	11.440	11.298	11.169	11.051	10.944	10.716	10.531	10.382	10.261	10.082	9.965	9.851	9.836	9.911
1	12.097	11.947	11.810	11.685	11.571	11.325	11.124	10.959	10.823	10.616	10.475	10.319	10.267	10.299
2	12.863	12.704	12.559	12.426	12.303	12.038	11.819	11.637	11.484	11.248	11.079	10.875	10.783	10.764
3	13.744	13.576	13.422	13.280	13.150	12.864	12.625	12.425	12.255	11.986	11.787	11.530	11.394	11.318
4	14.746	14.569	14.405	14.255	14.116	13.808	13.550	13.330	13.142	12.838	12.608	12.294	12.109	11.971
5	15.871	15.685	15.512	15.353	15.204	14.876	14.597	14.357	14.150	13.810	13.547	13.174	12.936	12.732
6	17.119	16.923	16.742	16.573	16.416	16.066	15.766	15.506	15.280	14.904	14.607	14.173	13.881	13.606
7	18.484	18.279	18.089	17.911	17.746	17.374	17.055	16.776	16.530	16.118	15.787	15.292	14.945	14.599
8	19.958	19.744	19.546	19.360	19.186	18.795	18.456	18.158	17.895	17.448	17.084	16.529	16.128	15.710
9	21.530	21.308	21.102	20.909	20.727	20.318	19.960	19.645	19.365	18.885	18.491	17.878	17.425	16.936
10	23.187	22.959	22.745	22.545	22.356	21.930	21.556	21.225	20.929	20.420	19.997	19.330	18.828	18.273
11	24.916	24.682	24.462	24.256	24.061	23.620	23.231	22.886	22.576	22.040	21.591	20.875	20.328	19.711
12	26.705	26.465	26.240	26.028	25.828	25.374	24.973	24.615	24.292	23.733	23.261	22.502	21.915	21.241
13	28.540	28.295	28.066	27.849	27.645	27.180	26.768	26.400	26.067	25.487	24.995	24.199	23.576	22.852

Table III

J (μ, M, ±4)

M	μ = 0.32	μ = 0.34	μ = 0.36	μ = 0.38	μ = 0.40	μ = 0.45	μ = 0.50	μ = 0.55	μ = 0.60	μ = 0.70	μ = 0.80	μ = 1.0	μ = 1.2	μ = 1.5
-∞	8.303	8.209	8.128	8.056	7.993	7.869	7.782	7.722	7.677	7.656	7.672	7.782	7.947	8.239
-30	8.307	8.214	8.132	8.060	7.997	7.873	7.785	7.725	7.687	7.659	7.675	7.784	7.950	8.241
-25	8.316	8.223	8.141	8.069	8.006	7.881	7.793	7.733	7.695	7.666	7.681	7.790	7.955	8.246
-20	8.345	8.251	8.169	8.096	8.033	7.907	7.818	7.757	7.718	7.688	7.702	7.808	7.972	8.261
-18	8.370	8.275	8.193	8.120	8.056	7.929	7.840	7.778	7.738	7.706	7.719	7.824	7.986	8.273
-16	8.409	8.314	8.230	8.157	8.093	7.964	7.873	7.810	7.769	7.736	7.747	7.849	8.009	8.293
-14	8.471	8.375	8.290	8.216	8.150	8.020	7.927	7.862	7.819	7.782	7.791	7.888	8.044	8.325
-12	8.568	8.470	8.384	8.308	8.241	8.107	8.010	7.942	7.897	7.855	7.860	7.950	8.101	8.375
-10	8.719	8.619	8.530	8.452	8.382	8.243	8.142	8.069	8.019	7.970	7.968	8.048	8.189	8.453
-9	8.824	8.722	8.631	8.551	8.481	8.337	8.232	8.157	8.104	8.050	8.043	8.115	8.251	8.508
-8	8.954	8.850	8.757	8.675	8.603	8.455	8.346	8.266	8.210	8.149	8.137	8.200	8.328	8.576
-7	9.116	9.009	8.913	8.829	8.754	8.601	8.486	8.402	8.342	8.273	8.254	8.305	8.424	8.661
-6	9.315	9.205	9.106	9.019	8.941	8.781	8.661	8.571	8.505	8.427	8.399	8.436	8.544	8.767
-5	9.560	9.445	9.344	9.253	9.171	9.003	8.875	8.778	8.706	8.616	8.578	8.599	8.693	8.899
-4	9.859	9.740	9.634	9.539	9.453	9.275	9.139	9.034	8.954	8.850	8.800	8.799	8.876	9.063
-3	10.222	10.098	9.986	9.886	9.796	9.607	9.460	9.345	9.256	9.136	9.071	9.046	9.102	9.265
-2	10.659	10.529	10.412	10.306	10.210	10.008	9.849	9.723	9.623	9.483	9.401	9.347	9.379	9.512
-1	11.181	11.044	10.920	10.808	10.706	10.489	10.316	10.177	10.065	9.903	9.801	9.712	9.716	9.815
0	11.798	11.654	11.523	11.404	11.295	11.061	10.872	10.718	10.593	10.405	10.280	10.152	10.123	10.181
1	12.519	12.367	12.228	12.101	11.984	11.732	11.526	11.356	11.215	11.000	10.849	10.677	10.610	10.622
2	13.351	13.190	13.042	12.907	12.782	12.511	12.287	12.099	11.942	11.695	11.517	11.295	11.187	11.146
3	14.296	14.126	13.970	13.826	13.693	13.401	13.158	12.952	12.777	12.498	12.290	12.015	11.861	11.763
4	15.354	15.175	15.010	14.857	14.716	14.404	14.141	13.917	13.723	13.411	13.171	12.841	12.639	12.479
5	16.519	16.332	16.158	15.997	15.847	15.515	15.233	14.990	14.779	14.432	14.162	13.775	13.523	13.298
6	17.784	17.588	17.406	17.238	17.080	16.729	16.428	16.167	15.938	15.559	15.257	14.814	14.512	14.222
7	19.139	18.935	18.746	18.569	18.404	18.035	17.716	17.438	17.194	16.783	16.452	15.954	15.603	15.248
8	20.575	20.364	20.168	19.984	19.812	19.426	19.091	18.797	18.537	18.097	17.738	17.188	16.791	16.373
9	22.087	21.869	21.666	21.476	21.298	20.896	20.545	20.237	19.962	19.494	19.109	18.511	18.069	17.591
10	23.670	23.446	23.236	23.040	22.856	22.439	22.074	21.752	21.464	20.970	20.560	19.916	19.432	18.897
11	25.320	25.090	24.875	24.673	24.483	24.053	23.675	23.339	23.038	22.520	22.087	21.399	20.876	20.287
12	27.033	26.798	26.578	26.371	26.175	25.732	25.342	24.994	24.682	24.140	23.685	22.958	22.397	21.757
13	28.803	28.563	28.337	28.126	27.926	27.471	27.069	26.710	26.387	25.825	25.350	24.585	23.990	23.302

Table III

$J(\mu, M, \pm 6)$

M	$\mu =$ 0.32	$\mu =$ 0.34	$\mu =$ 0.36	$\mu =$ 0.38	$\mu =$ 0.40	$\mu =$ 0.45	$\mu =$ 0.50	$\mu =$ 0.55	$\mu =$ 0.60	$\mu =$ 0.70	$\mu =$ 0.80	$\mu =$ 1.0	$\mu =$ 1.2	$\mu =$ 1.5
$-\infty$	8.303	8.209	8.128	8.056	7.993	7.869	7.782	7.722	7.677	7.656	7.672	7.782	7.947	8.239
-30	8.308	8.214	8.132	8.061	7.998	7.874	7.786	7.726	7.688	7.659	7.675	7.785	7.950	8.242
-25	8.319	8.225	8.143	8.071	8.008	7.883	7.795	7.735	7.697	7.668	7.683	7.792	7.957	8.248
-20	8.353	8.259	8.176	8.104	8.040	7.914	7.825	7.764	7.725	7.694	7.708	7.815	7.978	8.266
-18	8.382	8.287	8.204	8.132	8.068	7.941	7.851	7.789	7.749	7.717	7.729	7.834	7.995	8.282
-16	8.428	8.332	8.249	8.175	8.111	7.982	7.891	7.828	7.786	7.752	7.763	7.865	8.023	8.307
-14	8.500	8.404	8.319	8.245	8.179	8.048	7.954	7.889	7.846	7.808	7.816	7.913	8.068	8.347
-12	8.614	8.516	8.429	8.353	8.286	8.151	8.054	7.986	7.940	7.897	7.900	7.989	8.137	8.409
-10	8.792	8.691	8.602	8.523	8.454	8.313	8.211	8.137	8.087	8.035	8.031	8.108	8.247	8.507
-9	8.915	8.812	8.721	8.641	8.570	8.425	8.319	8.242	8.188	8.132	8.123	8.191	8.323	8.575
-8	9.068	8.963	8.870	8.787	8.714	8.564	8.454	8.373	8.315	8.251	8.236	8.294	8.418	8.660
-7	9.258	9.150	9.054	8.968	8.893	8.737	8.621	8.535	8.473	8.400	8.378	8.423	8.537	8.766
-6	9.491	9.380	9.281	9.192	9.113	8.951	8.828	8.736	8.667	8.585	8.553	8.583	8.684	8.898
-5	9.778	9.663	9.559	9.467	9.385	9.213	9.082	8.983	8.908	8.812	8.770	8.781	8.866	9.062
-4	10.128	10.008	9.900	9.803	9.716	9.535	9.394	9.286	9.202	9.092	9.036	9.024	9.091	9.264
-3	10.552	10.426	10.313	10.211	10.119	9.925	9.773	9.654	9.561	9.433	9.361	9.322	9.367	9.513
-2	11.061	10.929	10.809	10.701	10.603	10.396	10.231	10.100	9.995	9.846	9.755	9.685	9.703	9.816
-1	11.666	11.526	11.400	11.285	11.181	10.957	10.778	10.633	10.515	10.342	10.230	10.122	10.109	10.184
0	12.376	12.229	12.094	11.972	11.860	11.619	11.424	11.263	11.131	10.930	10.794	10.644	10.595	10.627
1	13.197	13.041	12.899	12.769	12.649	12.389	12.176	11.998	11.850	11.620	11.456	11.259	11.171	11.153
2	14.132	13.967	13.816	13.677	13.549	13.270	13.037	12.842	12.677	12.416	12.223	11.975	11.843	11.770
3	15.174	15.001	14.841	14.694	14.558	14.258	14.007	13.794	13.611	13.317	13.095	12.794	12.616	12.484
4	16.314	16.132	15.965	15.809	15.665	15.347	15.077	14.846	14.646	14.320	14.068	13.713	13.488	13.295
5	17.536	17.347	17.172	17.009	16.857	16.521	16.234	15.986	15.770	15.414	15.133	14.726	14.454	14.201
6	18.825	18.628	18.446	18.277	18.119	17.766	17.463	17.200	16.970	16.585	16.278	15.822	15.507	15.195
7	20.166	19.964	19.775	19.600	19.436	19.069	18.752	18.475	18.231	17.821	17.490	16.990	16.634	16.267
8	21.554	21.346	21.153	20.972	20.802	20.422	20.093	19.804	19.548	19.115	18.762	18.220	17.827	17.410
9	22.989	22.776	22.577	22.391	22.217	21.825	21.483	21.183	20.916	20.461	20.088	19.509	19.081	18.617
10	24.476	24.257	24.054	23.863	23.684	23.279	22.926	22.615	22.337	21.862	21.469	20.854	20.393	19.884
11	26.019	25.795	25.586	25.391	25.207	24.791	24.426	24.104	23.816	23.320	22.908	22.257	21.764	21.212
12	27.622	27.393	27.180	26.979	26.790	26.363	25.987	25.654	25.355	24.839	24.408	23.722	23.197	22.603
13	29.287	29.053	28.835	28.629	28.436	27.997	27.610	27.266	26.957	26.421	25.971	25.250	24.694	24.057

Table III

$J(\mu, M, \pm 8)$

M	μ = 0.32	μ = 0.34	μ = 0.36	μ = 0.38	μ = 0.40	μ = 0.45	μ = 0.50	μ = 0.55	μ = 0.60	μ = 0.70	μ = 0.80	μ = 1.0	μ = 1.2	μ = 1.5
$-\infty$	8.303	8.209	8.128	8.056	7.993	7.869	7.782	7.722	7.677	7.656	7.672	7.782	7.947	8.239
-30	8.309	8.215	8.134	8.062	7.999	7.875	7.787	7.727	7.689	7.660	7.676	7.786	7.951	8.243
-25	8.322	8.228	8.146	8.074	8.011	7.886	7.798	7.738	7.700	7.671	7.686	7.795	7.959	8.250
-20	8.363	8.269	8.186	8.114	8.050	7.924	7.835	7.774	7.734	7.703	7.717	7.823	7.986	8.274
-18	8.398	8.303	8.220	8.147	8.083	7.956	7.866	7.804	7.764	7.731	7.743	7.847	8.008	8.294
-16	8.453	8.357	8.274	8.200	8.135	8.007	7.915	7.851	7.810	7.775	7.785	7.886	8.044	8.326
-14	8.540	8.443	8.358	8.284	8.218	8.086	7.992	7.926	7.883	7.844	7.851	7.946	8.100	8.377
-12	8.677	8.578	8.491	8.415	8.347	8.212	8.114	8.045	7.998	7.954	7.955	8.042	8.188	8.457
-10	8.890	8.789	8.699	8.620	8.550	8.408	8.304	8.230	8.178	8.125	8.118	8.191	8.327	8.582
-9	9.038	8.935	8.843	8.762	8.690	8.544	8.436	8.358	8.303	8.243	8.232	8.295	8.423	8.669
-8	9.222	9.116	9.022	8.938	8.864	8.713	8.600	8.517	8.458	8.391	8.372	8.425	8.543	8.778
-7	9.449	9.340	9.243	9.157	9.080	8.922	8.803	8.715	8.650	8.574	8.547	8.586	8.692	8.913
-6	9.729	9.616	9.516	9.426	9.346	9.180	9.054	8.959	8.889	8.801	8.764	8.785	8.878	9.081
-5	10.073	9.955	9.851	9.757	9.673	9.498	9.363	9.260	9.182	9.080	9.031	9.031	9.106	9.289
-4	10.491	10.369	10.259	10.160	10.071	9.885	9.740	9.628	9.540	9.422	9.358	9.333	9.388	9.544
-3	10.997	10.868	10.753	10.648	10.554	10.355	10.198	10.074	9.976	9.838	9.757	9.701	9.731	9.857
-2	11.602	11.466	11.344	11.233	11.133	10.919	10.748	10.610	10.500	10.339	10.238	10.147	10.147	10.237
-1	12.317	12.174	12.044	11.926	11.818	11.587	11.401	11.248	11.124	10.937	10.812	10.681	10.647	10.694
0	13.149	12.998	12.860	12.734	12.619	12.369	12.165	11.996	11.856	11.640	11.489	11.313	11.240	11.239
1	14.100	13.940	13.794	13.660	13.536	13.267	13.044	12.858	12.701	12.454	12.275	12.048	11.933	11.878
2	15.165	14.996	14.841	14.698	14.566	14.277	14.035	13.831	13.656	13.378	13.169	12.889	12.729	12.616
3	16.326	16.149	15.986	15.835	15.695	15.387	15.126	14.904	14.713	14.402	14.164	13.832	13.625	13.453
4	17.563	17.378	17.207	17.049	16.902	16.575	16.298	16.060	15.852	15.512	15.245	14.863	14.611	14.381
5	18.848	18.657	18.480	18.315	18.161	17.820	17.528	17.275	17.054	16.687	16.395	15.967	15.673	15.388
6	20.161	19.964	19.782	19.612	19.453	19.099	18.794	18.529	18.296	17.906	17.593	17.124	16.795	16.460
7	21.489	21.288	21.101	20.926	20.763	20.398	20.083	19.808	19.565	19.156	18.825	18.321	17.960	17.582
8	22.831	22.626	22.435	22.257	22.090	21.715	21.391	21.106	20.855	20.429	20.082	19.548	19.159	18.743
9	24.193	23.984	23.789	23.607	23.437	23.053	22.720	22.428	22.168	21.727	21.365	20.804	20.389	19.938
10	25.584	25.371	25.173	24.987	24.813	24.421	24.079	23.779	23.511	23.054	22.678	22.090	21.652	21.168
11	27.016	26.799	26.596	26.407	26.229	25.828	25.477	25.168	24.892	24.420	24.029	23.414	22.951	22.436
12	28.497	28.276	28.069	27.876	27.694	27.283	26.923	26.605	26.320	25.832	25.425	24.783	24.295	23.746
13	30.036	29.810	29.599	29.401	29.215	28.794	28.424	28.097	27.803	27.297	26.874	26.202	25.688	25.105

Table III

$J(\mu, M, \pm 10)$

M	$\mu =$ 0.32	$\mu =$ 0.34	$\mu =$ 0.36	$\mu =$ 0.38	$\mu =$ 0.40	$\mu =$ 0.45	$\mu =$ 0.50	$\mu =$ 0.55	$\mu =$ 0.60	$\mu =$ 0.70	$\mu =$ 0.80	$\mu =$ 1.0	$\mu =$ 1.2	$\mu =$ 1.5
$-\infty$	8.303	8.209	8.128	8.056	7.993	7.869	7.782	7.722	7.677	7.656	7.672	7.782	7.947	8.239
-30	8.310	8.217	8.135	8.063	8.000	7.876	7.788	7.728	7.690	7.662	7.677	7.787	7.952	8.244
-25	8.326	8.232	8.150	8.078	8.015	7.890	7.802	7.742	7.703	7.674	7.689	7.798	7.963	8.253
-20	8.375	8.281	8.198	8.126	8.062	7.936	7.847	7.785	7.746	7.715	7.728	7.834	7.996	8.284
-18	8.417	8.322	8.239	8.166	8.102	7.975	7.884	7.822	7.782	7.749	7.761	7.864	8.024	8.310
-16	8.484	8.388	8.304	8.230	8.166	8.036	7.944	7.881	7.839	7.803	7.813	7.912	8.069	8.351
-14	8.588	8.492	8.406	8.331	8.265	8.133	8.039	7.973	7.928	7.889	7.895	7.989	8.140	8.416
-12	8.753	8.654	8.567	8.490	8.422	8.286	8.187	8.117	8.070	8.024	8.024	8.108	8.252	8.518
-10	9.011	8.908	8.818	8.738	8.668	8.525	8.420	8.344	8.291	8.235	8.227	8.296	8.428	8.678
-9	9.189	9.084	8.992	8.910	8.837	8.690	8.580	8.501	8.444	8.382	8.367	8.426	8.549	8.789
-8	9.410	9.303	9.208	9.123	9.048	8.895	8.780	8.696	8.634	8.564	8.542	8.588	8.701	8.928
-7	9.683	9.573	9.475	9.388	9.310	9.149	9.028	8.938	8.871	8.790	8.759	8.789	8.889	9.100
-6	10.020	9.906	9.804	9.713	9.632	9.463	9.334	9.236	9.162	9.069	9.027	9.038	9.122	9.314
-5	10.433	10.314	10.208	10.112	10.027	9.848	9.710	9.603	9.521	9.412	9.357	9.345	9.409	9.577
-4	10.935	10.811	10.699	10.599	10.508	10.317	10.167	10.050	9.958	9.832	9.760	9.720	9.761	9.900
-3	11.541	11.410	11.292	11.185	11.089	10.884	10.721	10.592	10.488	10.340	10.249	10.176	10.189	10.294
-2	12.263	12.125	12.000	11.886	11.782	11.561	11.384	11.240	11.123	10.950	10.837	10.725	10.706	10.769
-1	13.111	12.965	12.832	12.710	12.599	12.360	12.165	12.005	11.873	11.672	11.534	11.378	11.321	11.338
0	14.090	13.935	13.793	13.663	13.544	13.285	13.072	12.895	12.746	12.514	12.348	12.142	12.043	12.007
1	15.194	15.030	14.879	14.741	14.613	14.334	14.101	13.906	13.739	13.475	13.279	13.021	12.877	12.783
2	16.406	16.233	16.074	15.927	15.791	15.492	15.240	15.026	14.842	14.545	14.319	14.007	13.816	13.663
3	17.699	17.517	17.350	17.196	17.052	16.734	16.465	16.234	16.034	15.706	15.451	15.087	14.851	14.638
4	19.034	18.847	18.673	18.512	18.362	18.028	17.743	17.498	17.283	16.928	16.648	16.238	15.960	15.692
5	20.380	20.187	20.008	19.842	19.687	19.341	19.044	18.786	18.560	18.183	17.882	17.433	17.119	16.804
6	21.715	21.518	21.335	21.165	21.006	20.650	20.344	20.077	19.842	19.448	19.129	18.649	18.306	17.950
7	23.032	22.832	22.646	22.472	22.310	21.947	21.633	21.359	21.117	20.709	20.377	19.871	19.505	19.117
8	24.336	24.133	23.944	23.768	23.603	23.233	22.913	22.633	22.385	21.965	21.622	21.095	20.710	20.294
9	25.638	25.432	25.240	25.062	24.894	24.518	24.192	23.906	23.653	23.222	22.869	22.323	21.920	21.480
10	26.949	26.741	26.547	26.366	26.196	25.813	25.481	25.190	24.930	24.489	24.126	23.562	23.141	22.679
11	28.284	28.072	27.876	27.691	27.519	27.130	26.791	26.493	26.228	25.776	25.402	24.818	24.381	23.896
12	29.653	29.438	29.238	29.051	28.875	28.479	28.134	27.829	27.557	27.092	26.707	26.102	25.647	25.137
13	31.067	30.849	30.646	30.455	30.276	29.871	29.518	29.205	28.927	28.448	28.050	27.423	26.947	26.412

Table III

$J(\mu, M, \pm 12)$

M	$\mu =$ 0.32	$\mu =$ 0.34	$\mu =$ 0.36	$\mu =$ 0.38	$\mu =$ 0.40	$\mu =$ 0.45	$\mu =$ 0.50	$\mu =$ 0.55	$\mu =$ 0.60	$\mu =$ 0.70	$\mu =$ 0.80	$\mu =$ 1.0	$\mu =$ 1.2	$\mu =$ 1.5
$-\infty$	8.303	8.209	8.128	8.056	7.993	7.869	7.782	7.722	7.677	7.656	7.672	7.782	7.947	8.239
-30	8.311	8.218	8.136	8.064	8.002	7.877	7.789	7.730	7.691	7.663	7.679	7.788	7.953	8.245
-25	8.330	8.236	8.154	8.083	8.020	7.895	7.806	7.746	7.708	7.678	7.694	7.802	7.967	8.257
-20	8.389	8.295	8.212	8.140	8.076	7.950	7.860	7.799	7.759	7.728	7.741	7.846	8.008	8.295
-18	8.439	8.345	8.261	8.188	8.124	7.997	7.906	7.844	7.803	7.770	7.782	7.884	8.044	8.328
-16	8.519	8.423	8.339	8.265	8.200	8.071	7.979	7.914	7.872	7.836	7.846	7.944	8.100	8.380
-14	8.644	8.547	8.462	8.387	8.321	8.188	8.093	8.026	7.982	7.941	7.947	8.038	8.189	8.462
-12	8.841	8.742	8.654	8.577	8.509	8.372	8.273	8.202	8.154	8.106	8.106	8.187	8.329	8.591
-10	9.149	9.047	8.956	8.875	8.804	8.660	8.554	8.477	8.423	8.365	8.355	8.419	8.548	8.793
-9	9.362	9.257	9.164	9.082	9.008	8.859	8.748	8.667	8.609	8.544	8.527	8.581	8.699	8.933
-8	9.626	9.519	9.423	9.338	9.262	9.107	8.990	8.904	8.841	8.766	8.741	8.781	8.888	9.108
-7	9.954	9.842	9.743	9.655	9.576	9.413	9.290	9.197	9.128	9.042	9.007	9.030	9.123	9.325
-6	10.356	10.241	10.138	10.046	9.963	9.791	9.659	9.558	9.482	9.383	9.336	9.338	9.413	9.593
-5	10.850	10.729	10.621	10.524	10.437	10.254	10.113	10.002	9.917	9.801	9.740	9.716	9.770	9.923
-4	11.449	11.323	11.209	11.107	11.014	10.818	10.664	10.543	10.446	10.312	10.232	10.178	10.206	10.326
-3	12.171	12.037	11.917	11.808	11.709	11.498	11.330	11.195	11.086	10.928	10.828	10.737	10.734	10.817
-2	13.027	12.886	12.758	12.642	12.535	12.307	12.123	11.972	11.849	11.664	11.540	11.406	11.368	11.405
-1	14.028	13.878	13.742	13.617	13.503	13.255	13.053	12.885	12.745	12.530	12.378	12.197	12.117	12.103
0	15.172	15.013	14.868	14.734	14.611	14.343	14.121	13.935	13.778	13.530	13.348	13.114	12.989	12.917
1	16.445	16.277	16.122	15.980	15.848	15.559	15.317	15.112	14.936	14.655	14.442	14.153	13.980	13.847
2	17.817	17.639	17.476	17.325	17.185	16.876	16.615	16.392	16.199	15.884	15.641	15.298	15.078	14.884
3	19.241	19.056	18.886	18.728	18.580	18.254	17.976	17.737	17.529	17.185	16.914	16.521	16.257	16.006
4	20.671	20.480	20.304	20.140	19.987	19.647	19.356	19.104	18.884	18.516	18.223	17.789	17.487	17.186
5	22.070	21.875	21.695	21.527	21.370	21.020	20.720	20.458	20.228	19.843	19.533	19.067	18.736	18.394
6	23.422	23.225	23.041	22.871	22.711	22.355	22.047	21.779	21.542	21.144	20.822	20.332	19.979	19.606
7	24.730	24.531	24.345	24.173	24.011	23.649	23.336	23.063	22.822	22.414	22.083	21.575	21.205	20.809
8	26.006	25.804	25.617	25.443	25.279	24.913	24.596	24.319	24.073	23.658	23.319	22.797	22.414	21.999
9	27.262	27.059	26.870	26.694	26.529	26.159	25.838	25.557	25.307	24.885	24.539	24.004	23.609	23.178
10	28.514	28.309	28.118	27.940	27.774	27.399	27.074	26.789	26.536	26.106	25.753	25.206	24.800	24.353

Table III

$J(\mu, M, \pm 14)$

M	$\mu =$ 0.32	$\mu =$ 0.34	$\mu =$ 0.36	$\mu =$ 0.38	$\mu =$ 0.40	$\mu =$ 0.45	$\mu =$ 0.50	$\mu =$ 0.55	$\mu =$ 0.60	$\mu =$ 0.70	$\mu =$ 0.80	$\mu =$ 1.0	$\mu =$ 1.2	$\mu =$ 1.5
$-\infty$	8.303	8.209	8.128	8.056	7.993	7.869	7.782	7.722	7.677	7.656	7.672	7.782	7.947	8.239
-30	8.313	8.219	8.138	8.066	8.003	7.879	7.791	7.731	7.693	7.664	7.680	7.789	7.955	8.246
-25	8.335	8.241	8.159	8.087	8.024	7.899	7.811	7.751	7.712	7.683	7.698	7.807	7.971	8.261
-20	8.405	8.310	8.228	8.155	8.092	7.965	7.875	7.814	7.774	7.743	7.756	7.861	8.022	8.309
-18	8.464	8.369	8.286	8.213	8.149	8.021	7.930	7.868	7.827	7.793	7.805	7.907	8.066	8.350
-16	8.558	8.462	8.378	8.304	8.239	8.109	8.017	7.952	7.910	7.874	7.882	7.980	8.135	8.414
-14	8.706	8.609	8.523	8.448	8.382	8.249	8.153	8.086	8.041	8.000	8.005	8.095	8.244	8.516
-12	8.939	8.839	8.752	8.674	8.606	8.468	8.368	8.296	8.247	8.199	8.197	8.276	8.416	8.675
-10	9.303	9.200	9.108	9.028	8.956	8.811	8.703	8.625	8.570	8.510	8.498	8.560	8.685	8.926
-9	9.555	9.449	9.355	9.272	9.198	9.048	8.936	8.853	8.794	8.726	8.707	8.756	8.871	9.099
-8	9.867	9.758	9.662	9.576	9.500	9.343	9.224	9.136	9.072	8.994	8.966	9.001	9.103	9.315
-7	10.254	10.142	10.042	9.952	9.873	9.708	9.582	9.487	9.416	9.327	9.288	9.304	9.390	9.583
-6	10.730	10.614	10.509	10.416	10.332	10.158	10.023	9.920	9.840	9.737	9.685	9.678	9.745	9.914
-5	11.313	11.191	11.082	10.983	10.895	10.708	10.563	10.449	10.361	10.239	10.172	10.137	10.180	10.320
-4	12.021	11.893	11.777	11.673	11.578	11.378	11.220	11.094	10.994	10.852	10.765	10.697	10.712	10.816
-3	12.871	12.736	12.613	12.502	12.400	12.184	12.011	11.871	11.751	11.590	11.481	11.373	11.355	11.416
-2	13.878	13.734	13.603	13.484	13.375	13.141	12.950	12.793	12.664	12.468	12.332	12.179	12.122	12.134
-1	15.047	14.894	14.755	14.627	14.509	14.254	14.044	13.870	13.723	13.494	13.330	13.124	13.023	12.979
0	16.373	16.210	16.061	15.924	15.797	15.521	15.290	15.096	14.930	14.667	14.471	14.210	14.060	13.954
1	17.826	17.654	17.496	17.349	17.214	16.916	16.664	16.451	16.267	15.969	15.740	15.422	15.222	15.053
2	19.360	19.179	19.012	18.857	18.714	18.396	18.126	17.894	17.693	17.363	17.104	16.732	16.485	16.253
3	20.911	20.723	20.550	20.389	20.239	19.905	19.620	19.373	19.158	18.800	18.516	18.097	17.808	17.522
4	22.424	22.232	22.053	21.887	21.733	21.388	21.091	20.834	20.608	20.230	19.927	19.472	19.151	18.820
5	23.866	23.671	23.489	23.320	23.162	22.810	22.506	22.241	22.008	21.617	21.300	20.821	20.476	20.113
6	25.232	25.035	24.851	24.680	24.520	24.163	23.854	23.585	23.347	22.947	22.621	22.125	21.763	21.378

Table III

$J(\mu, M, \pm 16)$

M	$\mu =$ 0.32	$\mu =$ 0.34	$\mu =$ 0.36	$\mu =$ 0.38	$\mu =$ 0.40	$\mu =$ 0.45	$\mu =$ 0.50	$\mu =$ 0.55	$\mu =$ 0.60	$\mu =$ 0.70	$\mu =$ 0.80	$\mu =$ 1.0	$\mu =$ 1.2	$\mu =$ 1.5
$-\infty$	8.303	8.209	8.128	8.056	7.993	7.869	7.782	7.722	7.677	7.656	7.672	7.782	7.947	8.239
-30	8.315	8.221	8.139	8.068	8.005	7.880	7.793	7.733	7.695	7.666	7.682	7.791	7.956	8.248
-25	8.340	8.247	8.165	8.093	8.030	7.905	7.816	7.756	7.718	7.688	7.703	7.812	7.976	8.266
-20	8.422	8.327	8.244	8.172	8.108	7.982	7.892	7.830	7.791	7.759	7.772	7.876	8.038	8.324
-18	8.491	8.396	8.312	8.239	8.175	8.047	7.956	7.894	7.853	7.819	7.830	7.932	8.090	8.373
-16	8.600	8.504	8.420	8.346	8.281	8.151	8.058	7.993	7.951	7.914	7.922	8.019	8.174	8.452
-14	8.773	8.675	8.590	8.514	8.448	8.314	8.218	8.151	8.106	8.064	8.068	8.157	8.305	8.575
-12	9.044	8.944	8.856	8.779	8.710	8.572	8.471	8.399	8.349	8.300	8.297	8.374	8.512	8.769
-10	9.468	9.365	9.273	9.192	9.120	8.974	8.866	8.787	8.731	8.669	8.656	8.714	8.836	9.073
-9	9.762	9.656	9.562	9.478	9.404	9.252	9.139	9.055	8.994	8.925	8.903	8.949	9.060	9.283
-8	10.126	10.017	9.920	9.834	9.757	9.598	9.478	9.389	9.323	9.243	9.212	9.241	9.339	9.545
-7	10.578	10.465	10.364	10.274	10.193	10.026	9.899	9.802	9.729	9.637	9.595	9.604	9.685	9.870
-6	11.134	11.016	10.911	10.816	10.732	10.555	10.418	10.312	10.231	10.123	10.067	10.052	10.112	10.270
-5	11.814	11.691	11.580	11.481	11.391	11.201	11.053	10.937	10.845	10.718	10.645	10.601	10.635	10.762
-4	12.640	12.510	12.393	12.287	12.191	11.987	11.825	11.696	11.592	11.443	11.350	11.269	11.273	11.362
-3	13.630	13.493	13.368	13.255	13.152	12.931	12.753	12.609	12.490	12.315	12.197	12.074	12.042	12.085
-2	14.800	14.654	14.521	14.399	14.288	14.048	13.851	13.699	13.554	13.348	13.203	13.031	12.956	12.945
-1	16.153	15.997	15.854	15.723	15.603	15.341	15.124	14.943	14.790	14.549	14.372	14.145	14.023	13.952
0	17.671	17.505	17.352	17.212	17.082	16.798	16.559	16.357	16.185	15.908	15.698	15.412	15.239	15.103
1	19.312	19.136	18.974	18.825	18.686	18.379	18.120	17.898	17.707	17.394	17.151	16.806	16.582	16.380
2	21.007	20.823	20.653	20.495	20.348	20.023	19.745	19.506	19.298	18.953	18.681	18.283	18.012	17.748
3	22.676	22.486	22.310	22.146	21.993	21.653	21.362	21.110	20.888	20.519	20.224	19.783	19.474	19.158
4	24.260	24.065	23.885	23.718	23.562	23.212	22.912	22.650	22.420	22.035	21.723	21.252	20.915	20.562

Table III

J (μ, M, ±18)

M	μ = 0.32	μ = 0.34	μ = 0.36	μ = 0.38	μ = 0.40	μ = 0.45	μ = 0.50	μ = 0.55	μ = 0.60	μ = 0.70	μ = 0.80	μ = 1.0	μ = 1.2	μ = 1.5
-∞	8.303	8.209	8.128	8.056	7.993	7.869	7.782	7.722	7.677	7.656	7.672	7.782	7.947	8.239
-30	8.316	8.223	8.141	8.069	8.007	7.882	7.794	7.734	7.696	7.668	7.683	7.793	7.958	8.249
-25	8.346	8.252	8.170	8.098	8.035	7.910	7.822	7.762	7.723	7.694	7.709	7.817	7.981	8.271
-20	8.439	8.345	8.262	8.190	8.126	7.999	7.909	7.848	7.808	7.776	7.789	7.893	8.054	8.340
-18	8.519	8.424	8.340	8.267	8.203	8.075	7.984	7.921	7.880	7.846	7.857	7.958	8.117	8.399
-16	8.645	8.549	8.464	8.390	8.325	8.195	8.102	8.037	7.994	7.957	7.965	8.061	8.215	8.492
-14	8.843	8.745	8.659	8.584	8.517	8.384	8.287	8.220	8.174	8.132	8.135	8.223	8.371	8.639
-12	9.155	9.055	8.966	8.889	8.820	8.681	8.580	8.507	8.457	8.407	8.403	8.479	8.615	8.870
-10	9.643	9.539	9.447	9.366	9.293	9.146	9.037	8.958	8.901	8.838	8.823	8.879	8.998	9.232
-9	9.981	9.874	9.780	9.696	9.621	9.468	9.354	9.270	9.208	9.137	9.114	9.156	9.264	9.483
-8	10.400	10.291	10.193	10.106	10.029	9.869	9.748	9.657	9.590	9.508	9.475	9.500	9.594	9.795
-7	10.920	10.807	10.705	10.615	10.533	10.365	10.236	10.138	10.063	9.968	9.923	9.927	10.003	10.181
-6	11.561	11.443	11.336	11.241	11.156	10.977	10.838	10.730	10.647	10.535	10.476	10.454	10.508	10.658
-5	12.345	12.221	12.109	12.009	11.918	11.726	11.575	11.456	11.362	11.231	11.154	11.101	11.127	11.243
-4	13.297	13.166	13.047	12.940	12.843	12.636	12.471	12.338	12.231	12.076	11.977	11.886	11.881	11.955
-3	14.438	14.299	14.172	14.057	13.952	13.728	13.546	13.397	13.275	13.092	12.967	12.831	12.787	12.812
-2	15.782	15.634	15.498	15.375	15.261	15.016	14.814	14.647	14.508	14.292	14.138	13.950	13.860	13.829
-1	17.329	17.170	17.025	16.892	16.769	16.501	16.278	16.090	15.932	15.680	15.493	15.246	15.106	15.010
0	19.050	18.881	18.726	18.582	18.450	18.158	17.913	17.704	17.525	17.235	17.014	16.705	16.512	16.347
1	20.883	20.704	20.539	20.386	20.245	19.931	19.664	19.436	19.237	18.911	18.656	18.288	18.042	17.810
2	22.734	22.547	22.375	22.214	22.065	21.733	21.449	21.203	20.989	20.632	20.349	19.929	19.637	19.345
3	24.510	24.317	24.139	23.974	23.819	23.474	23.178	22.921	22.695	22.316	22.012	21.553	21.227	20.887
4	26.151	25.955	25.774	25.606	25.448	25.096	24.792	24.528	24.295	23.903	23.585	23.102	22.753	22.382

Table III

$J(\mu, M, \pm 20)$

M	$\mu =$ 0.32	$\mu =$ 0.34	$\mu =$ 0.36	$\mu =$ 0.38	$\mu =$ 0.40	$\mu =$ 0.45	$\mu =$ 0.50	$\mu =$ 0.55	$\mu =$ 0.60	$\mu =$ 0.70	$\mu =$ 0.80	$\mu =$ 1.0	$\mu =$ 1.2	$\mu =$ 1.5
$-\infty$	8.303	8.209	8.128	8.056	7.993	7.869	7.782	7.722	7.677	7.656	7.672	7.782	7.947	8.239
-30	8.318	8.225	8.143	8.071	8.009	7.884	7.796	7.736	7.698	7.669	7.685	7.794	7.960	8.251
-25	8.352	8.258	8.176	8.104	8.041	7.916	7.828	7.767	7.729	7.699	7.714	7.822	7.987	8.277
-20	8.458	8.363	8.280	8.208	8.144	8.017	7.928	7.866	7.826	7.794	7.807	7.911	8.072	8.358
-18	8.548	8.453	8.369	8.296	8.232	8.104	8.013	7.950	7.909	7.875	7.885	7.986	8.144	8.426
-16	8.691	8.595	8.510	8.436	8.371	8.240	8.147	8.082	8.039	8.002	8.010	8.105	8.259	8.535
-14	8.916	8.818	8.732	8.656	8.590	8.456	8.359	8.292	8.246	8.203	8.206	8.293	8.440	8.707
-12	9.270	9.170	9.081	9.003	8.934	8.795	8.694	8.621	8.570	8.520	8.515	8.589	8.724	8.978
-10	9.824	9.720	9.628	9.546	9.474	9.326	9.217	9.137	9.079	9.015	8.999	9.053	9.171	9.402
-9	10.208	10.102	10.007	9.923	9.848	9.694	9.579	9.494	9.432	9.359	9.334	9.374	9.480	9.695
-8	10.686	10.576	10.478	10.391	10.313	10.152	10.030	9.938	9.870	9.786	9.752	9.774	9.864	10.060
-7	11.278	11.163	11.061	10.970	10.889	10.719	10.589	10.489	10.414	10.316	10.269	10.269	10.341	10.513
-6	12.007	11.888	11.781	11.685	11.599	11.418	11.278	11.169	11.084	10.969	10.907	10.880	10.929	11.072
-5	12.900	12.775	12.663	12.561	12.469	12.275	12.123	12.002	11.906	11.770	11.690	11.630	11.650	11.757
-4	13.985	13.852	13.733	13.625	13.526	13.316	13.149	13.013	12.904	12.744	12.640	12.540	12.526	12.590
-3	15.284	15.143	15.016	14.899	14.793	14.564	14.379	14.227	14.102	13.912	13.782	13.634	13.579	13.590
-2	16.813	16.662	16.525	16.400	16.284	16.034	15.829	15.657	15.514	15.290	15.128	14.926	14.823	14.774
-1	18.564	18.403	18.256	18.120	17.995	17.721	17.493	17.300	17.137	16.875	16.679	16.415	16.259	16.141
0	20.496	20.325	20.167	20.021	19.885	19.588	19.336	19.122	18.937	18.636	18.404	18.076	17.864	17.675
1	22.523	22.341	22.174	22.018	21.874	21.554	21.281	21.046	20.842	20.505	20.239	19.850	19.586	19.328
2	24.524	24.335	24.160	23.998	23.846	23.508	23.219	22.968	22.749	22.382	22.089	21.651	21.342	21.026
3	26.393	26.199	26.019	25.852	25.696	25.347	25.047	24.786	24.556	24.171	23.859	23.387	23.047	22.689
4	28.079	27.883	27.701	27.532	27.373	27.019	26.713	26.446	26.211	25.815	25.493	25.001	24.643	24.259

Appendix II

Derivation of the Spectrum $S(\vec{k})$ Corresponding to the Correlation Function $\{2^{1-\mu}/\Gamma(\mu)\}(r/\ell_o)^{\mu} K_{\mu}(r/\ell_o)$

In this appendix it will be shown that $S(\vec{k})$ is given by (8) for a correlation function having the form (6). By definition

$$S(\vec{k}) \equiv \int\int\int_{-\infty}^{+\infty} \cos(\vec{k} \cdot \vec{r})\, C(r/\ell_o)\, dx\, dy\, dz \tag{II-1}$$

where

$$\vec{r} \equiv x\vec{a} + y\vec{b} + z\vec{c} = r\vec{r}_1 \tag{II-2}$$

$$\vec{k} \equiv k_p\vec{a} + k_n\vec{b} + k_v\vec{c} = k\vec{k}_1 \tag{II-3}$$

The characteristic scale ℓ_o is defined by (7) or by the following:

$$\vec{\rho} \equiv \frac{x}{\ell_p}\vec{a} + \frac{y}{\ell_n}\vec{b} + \frac{z}{\ell_v}\vec{c} = (r/\ell_o)\vec{\rho}_1 = \rho\vec{\rho}_1 \tag{II-4}$$

It will be convenient also to define a vector $\vec{q}$:

$$\vec{q} = \ell_p k_p \vec{a} + \ell_n k_n \vec{b} + \ell_v k_v \vec{c} \equiv \ell_k k \vec{q}_1 \tag{II-5}$$

With this notation

$$\vec{k} \cdot \vec{r} = \vec{q} \cdot \vec{\rho} = xk_p + yk_n + zk_v \tag{II-6}$$

Let $\rho_1 = x/\ell_p$, $\rho_2 = y/\ell_n$ and $\rho_3 = z/\ell_v$; then (II-1) may be expressed:

$$S(\vec{k}) = \ell_p \ell_n \ell_v \int\int\int_{-\infty}^{+\infty} \cos(\vec{q} \cdot \vec{\rho})\, C(\rho)\, d\rho_1\, d\rho_2\, d\rho_3 \qquad \text{(II-7)}$$

If we now choose the spherical polar coordinate system, ρ, ϕ, θ with $\vec{q}_1$ in the direction of the polar axis so that $\vec{q}_1 \cdot \vec{\rho}_1 = \cos\phi$, then (II-7) becomes

$$S(\vec{k}) = \ell_p \ell_n \ell_v \int_0^{\infty}\int_0^{\pi}\int_0^{2\pi} \cos(q\rho\cos\phi)\, C(\rho)\, \rho^2 \sin\phi\, d\theta\, d\phi\, d\rho \qquad \text{(II-8)}$$

When we note that

$$\sin\phi \cos(q\,\rho\cos\phi) = -\frac{1}{q\rho}\frac{d}{d\theta}\sin(\rho q \cos\phi)$$

we may perform the integrations with respect to θ and ϕ:

$$S(\vec{k}) = \frac{4\pi \ell_p \ell_n \ell_v}{q} \int_0^{\infty} \rho \sin(\rho q)\, C(\rho)\, d\rho \qquad \text{(II-9)}$$

With $C(\rho)$ defined by (6) the above integration may be performed and the result is given by (8).

The reader should be cautioned that this particular form of correlation function is not necessarily the correct function for describing the characteristics of the atmosphere. However, measured atmospheric spectra do tend to behave qualitatively, i.e.,decrease inversely as some power of k, at least for large wave numbers, in the manner illustrated on Fig. 4. The author is not aware of any information which would lead one to believe that anisotropy, if it exists at all, may be described by the particular ellipsoidal scale length anisotropy described by (6), (7), (8) and (9); in particular it seems not unlikely that the slope $[-(2\mu + 3)]$ of the spectrum $S(\vec{k})$ may depend on the direction of $\vec{k}$. Nevertheless it is believed that this particular model is useful for describing one possible way in which the slope of the spectrum $S(\vec{k})$ and anisotropy may enter into the various measurable quantities involved in the theory. It seems particularly desirable to have a model in view of the difficulty of forming any intuitive feeling for the nature of $S(\vec{k})$ and the practical impossibility of directly measuring its magnitude. The nearest approach to a direct measurement of $S(\vec{k})$ involves measurements of the structure function--see (14)--but this is only valid over a limited range of k and then only for isotropic media; furthermore the derivation of (14) depends upon assuming the particular form (6) for the correlation function, and the function of μ in (14) derives entirely from this form of correlation function.

An interesting discussion of the fundamental differences between one dimensional and three dimensional spectra is given in a recent note by Gifford.[20]

Table IV is a tabulation of $C(r/\ell_o)$ for several values of μ which may prove to be useful:

Table IV

Short Table of the Correlation Function

$$C(\vec{r}) \equiv \{2^{1-\mu}/\Gamma(\mu)\}(r/\ell_o)^{\mu} K_{\mu}(r/\ell_o)$$

(r/ℓ_o)	$\mu = 1/3$	$\mu = 1/2$	$\mu = 2/3$	$\mu = 1$	$\mu = 3/2$
0.001	0.99044762	0.99900050	0.99988298	0.99999624	0.99999950
0.002	0.98483745	0.99800200	0.99970625	0.99998634	0.99999800
0.003	0.98013282	0.99700450	0.99949720	0.99997109	0.99999551
0.005	0.97207684	0.99501248	0.99901185	0.99992607	0.99998754
0.007	0.96506163	0.99302444	0.99845978	0.99986334	0.99997561
0.01	0.95569674	0.99004983	0.99753775	0.99973894	0.99995033
0.018	0.93450651	0.98216103	0.99468727	0.99924936	0.99983993
0.02	0.92975947	0.98019867	0.99390624	0.99909436	0.99980265
0.03	0.90809119	0.97044553	0.98969568	0.99814463	0.99955890
0.05	0.87122615	0.95122942	0.98017441	0.99548372	0.99879090
0.07	0.83943571	0.93239382	0.96967707	0.99196974	0.99766139
0.1	0.79755899	0.90483742	0.95276233	0.98538448	0.99532116
0.2	0.68589016	0.81873075	0.89154336	0.95519450	0.98247690
0.3	0.59862209	0.74081822	0.82835332	0.91679760	0.96306369
0.5	0.46514732	0.60653066	0.70684216	0.82822055	0.90979599
0.7	0.36646271	0.49658530	0.59766997	0.73519848	0.84419502
1.0	0.25979142	0.36787944	0.46007775	0.60190723	0.73575888

For numerical work, the following expressions for the correlation function $C(\rho, \mu) \equiv \{2/\Gamma(\mu)\}(\rho/2)^{\mu} K_{\mu}(\rho)$ are useful:

$$C(\rho,\ 0.5) = \exp[-\rho] \tag{II-10}$$

$$C(\rho,\ 1.5) = (1 + \rho)\exp[-\rho] \tag{II-11}$$

$$C(\rho, \mu) = \Gamma(1 - \mu)(\rho/2)^{\mu}\{I_{-\mu}(\rho) - I_{\mu}(\rho)\} \tag{II-12}$$

where $I_{\mu}(\rho)$ is the modified Bessel function of the first kind.

$$I_{\mu}(\rho) = \sum_{r=0}^{\infty} \frac{(\rho/2)^{\mu + 2r}}{r!\,\Gamma(1 + \mu + r)} \tag{II-13}$$

$$C(\rho,\mu) = \sum_{r=0}^{\infty} \frac{(\rho/2)^{2r}\,\Gamma(1 - \mu)}{r!\,\Gamma(1 - \mu + r)}\left[1 - \frac{\Gamma(1 - \mu + r)}{\Gamma(1 + \mu + r)}\left(\frac{\rho}{2}\right)^{2\mu}\right] \tag{II-14}$$

When $0 < \mu < 2$ and $\mu \neq 1$, the leading terms in (II-14) are:

$$C(\rho,\mu) = 1 - \frac{\Gamma(1 - \mu)}{\Gamma(1 + \mu)}\left(\frac{\rho}{2}\right)^{2\mu} + \frac{1}{1 - \mu}\left(\frac{\rho}{2}\right)^{2} - \frac{\Gamma(1 - \mu)}{(1 + \mu)\,\Gamma(1 + \mu)}\left(\frac{\rho}{2}\right)^{2\mu + 2} + \frac{1}{2(1 - \mu)(2 - \mu)}\left(\frac{\rho}{2}\right)^{4} - \ldots \tag{II-15}$$

When $\mu = 1$ the following series may be used:

$$C(\rho,\ 1) = 1 + 2[\gamma - 0.5 + \ln(\rho/2)](\rho/2)^{2} + [\gamma - 1.25 + \ln(\rho/2)](\rho/2)^{4} + \ldots \tag{II-16}$$

where $\gamma = 0.5772156649$.

Bessel function tables which have been found useful in this application are:

(1) British Association Mathematical Tables

Vol. VI Bessel Functions Part I, Functions of Orders Zero and Unity (1937)

and Vol. X Bessel Functions Part II, Functions of Positive Integer Order 2 to 20 (1952)

Published for the Royal Society at the Cambridge University Press

(2) Tables of Bessel Functions of Fractional Order

Volumes I and II, Prepared by the Computation Laboratory of the National Applied Mathematics Laboratories of the National Bureau of Standards, Columbia University Press, New York, 1948

In particular, $K_1(\rho)$ is tabulated in reference (1), Vol. VI and $I_{-1/3}(\rho)$, $I_{+1/3}(\rho)$, $I_{-2/3}(\rho)$ and $I_{+2/3}(\rho)$ are tabulated in reference 2, Vol. II.

Appendix III

Carrier Frequency Dependence of the Basic Transmission Loss by Regression Analysis

By using first the 1955[10] and then the 1958[5] prediction formulas, the basic transmission loss was calculated for 98 transmission paths for which reliable winter afternoon observations were available, and $\Delta_i = L_{bms}$ (Calculated) - L_{bms} (Observed) was determined for each of these paths. These 98 values of Δ_i were then fitted by least squares to the following formula:

$$\Delta = a + b \log_{10} f_{Mc} \qquad \text{(III-1)}$$

These 98 paths covered a frequency range from 65.8 to 4090 Mc. Using the 1955 formula this regression analysis indicated $b = -6.01 \pm 5.77$, whereas the 1958 formula resulted in $b = -2.50 \pm 5.53$. Since the 1955 and 1958 prediction formulas were both based on the assumption that $\mu = 1$, it follows from the above analysis that $(2\bar{\mu} + 1)10 = 36.01 \pm 5.77$ using the 1955 formula, and that $(2\bar{\mu} + 1)10 = 32.50 \pm 5.53$ using the 1958 formula, i.e., $\bar{\mu} = 1.3005 \pm 0.2885$ or $\bar{\mu} = 1.125 \pm 0.2765$, respectively.

Fig. 8 compares the basic transmission losses predicted by these two formulas, and it is clear from this figure that the 1955

COMPARISON OF MEDIAN BASIC TRANSMISSION LOSS PREDICTIONS BY NBS 1955 AND 1958 FORMULAS

$f = 100$ Mc; $h_{te} = 500$ FEET (152.4 METERS)

$h_{re} = 30$ FEET (9.144 METERS) $N_s = 301$

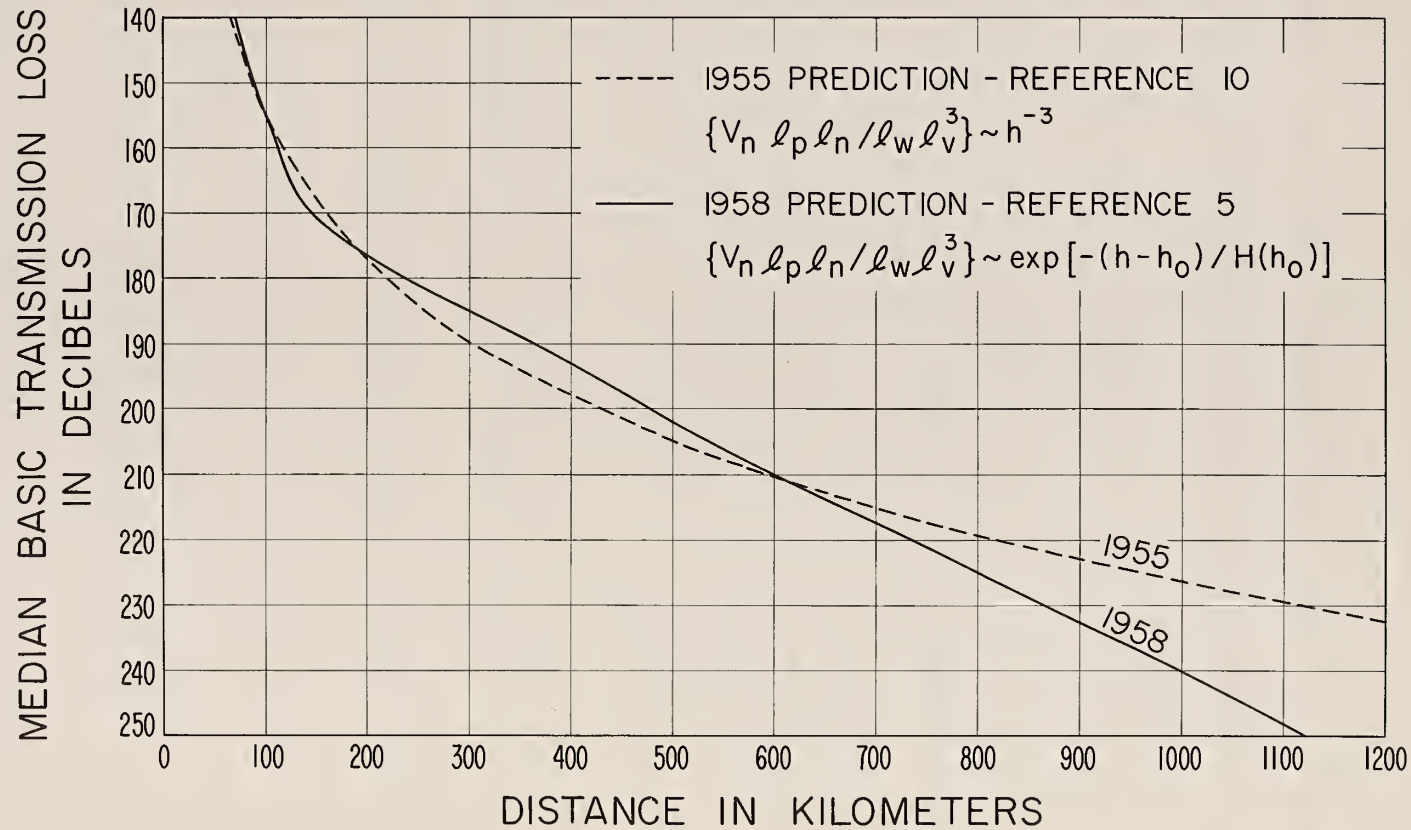

Figure 8

formula indicates much less loss at distances greater than 800 km than the 1958 formula. Since the data agree somewhat better, particularly at these larger distances, with the 1958 formula, the above regression analyses were confined to the 98 paths for which d(miles) θ(radians) $\leq$ 35.

It appears from this analysis and the fact that $(2\bar{\mu} + 1)10 = 33.1 \pm 5.55$ when all 105 paths are used with the 1958 prediction formula, that the higher frequencies may be subject to a somewhat greater loss than is predicted by using $\mu = 1$. Some, if not all, of this additional loss may be attributed to the fact that our theory postulates that ground reflection at the transmitting and receiving ends of the path quadruples ($\bar{g}_t \bar{g}_r = 4$) the available scattered power at the receiver. It seems likely that $\bar{g}_t \bar{g}_r$ will be less than 4 and may approach 2 or less at the higher frequencies, at least for propagation over land paths.

References

1. Ralph Bolgiano, "Wavelength dependence in transhorizon propagation," Letter to the Editor, Proc. I. R. E. 47, 331 (1959).

2. K. A. Norton, "System loss in radio wave propagation," J. Res. NBS 63D, 53 (1959).

3. W. J. Hartman and R. E. Wilkerson, "Path antenna gain in an exponential atmosphere," J. Res. NBS 63D, 273 (1959).

4. K. A. Norton, P. L. Rice and L. E. Vogler, "The use of angular distance in estimating transmission loss and fading range for propagation through a turbulent atmosphere over irregular terrain," Proc. I. R. E. 43, 1488 (1955).

5. P. L. Rice, A. G. Longley and K. A. Norton, "Prediction of the cumulative distribution with time of ground wave and tropospheric wave transmission loss," NBS Technical Note No. 15, Available at a cost of $1.50 from the Office of Technical Services, U.S. Department of Commerce, Washington, D.C.

6. F. Villars and V. F. Weisskopf, "On the scattering of radio waves by turbulent fluctuations of the atmosphere," Proc. I. R. E. 43, 1232 (1955).

7. A. D. Wheelon, "Spectrum of turbulent fluctuations produced by convective mixing of gradients," Phys. Rev. 105, 1706 (1957).

8. A. D. Wheelon, "Radio-wave scattering by tropospheric irregularities," J. Res. NBS 63D, 205 (1959).

9. A. P. Barsis, "Comparative 100 Mc measurements at distances far beyond the radio horizon," Convention Record I. R. E. 2, Part 1 - Antennas and Propagation (1954).

10. K. A. Norton, "Point-to-point radio relaying via the scatter mode of tropospheric propagation," I. R. E. Trans. on Commun. Systems CS-4, no. 1, 39 (1956).

11. B. R. Bean and G. D. Thayer, "On models of the atmospheric radio refractive index," Proc. I. R. E. 47, 740 (1959).

12. R. A. Fisher, "On the probable error of a coefficient of correlation deduced from a small sample," Metron 1, no. 4 (1921).

13. A. Hald, "Statistical theory with engineering applications," John Wiley and Sons, 1952.

14. K. A. Norton, "Recent experimental evidence favoring the $\rho K_1(\rho)$ correlation function for describing the turbulence of refractivity in the troposphere and stratosphere," Report given at the Joint Commissions on the Ionosphere and on Radio Meteorology held under the auspices of the International Scientific Radio Union at New York University, August, 1957; J. Atmospheric and Terrest. Phys. 15, 206 (1959).

15. K. A. Norton et al, "Radio Studies of Atmospheric Turbulence," Vol. I and Vol. II, to be published as an NBS Technical Note.

16. M. C. Thompson, H. B. Janes, and A. W. Kirkpatrick, "An analysis of time variations in atmospheric refractive index and apparent radio path length," J. Geophys. Res. 65, 193 (1960).

17. J. W. Herbstreit, K. A. Norton, P. L. Rice and G. E. Schafer, "Radio Wave Scattering in Tropospheric Propagation," I. R. E. Convention Record, Part 2, Antennas and Communications, 85 (1953).

18. Earl E. Gossard, "Atmospheric spectra and trans-horizon microwave fields," Proc. 7th Weather Radar Conference, Miami Beach, Florida, Nov. 17-20, 1958.

19. Frank Gifford, Jr., "The relation between space and time correlations in the atmosphere," J. Meteorol. 13, 289 (1956).

20. Frank Gifford, "The interpretation of meteorological spectra and correlations," J. Meteorol. 16, 343 (1959).

U.S. DEPARTMENT OF COMMERCE
Frederick H. Mueller, *Secretary*

NATIONAL BUREAU OF STANDARDS
A. V. Astin, *Director*

THE NATIONAL BUREAU OF STANDARDS

The scope of activities of the National Bureau of Standards at its major laboratories in Washington, D.C., and Boulder, Colorado, is suggested in the following listing of the divisions and sections engaged in technical work. In general, each section carries out specialized research, development, and engineering in the field indicated by its title. A brief description of the activities, and of the resultant publications, appears on the inside of the front cover.

WASHINGTON, D.C.

Electricity and Electronics. Resistance and Reactance. Electron Devices. Electrical Instruments. Magnetic Measurements. Dielectrics. Engineering Electronics. Electronic Instrumentation. Electrochemistry.

Optics and Metrology. Photometry and Colorimetry. Photographic Technology. Length. Engineering Metrology.

Heat. Temperature Physics. Thermodynamics. Cryogenic Physics. Rheology. Molecular Kinetics. Free Radicals Research.

Atomic and Radiation Physics. Spectroscopy. Radiometry. Mass Spectrometry. Solid State Physics. Electron Physics. Atomic Physics. Neutron Physics. Radiation Theory. Radioactivity. X-rays. High Energy Radiation. Nucleonic Instrumentation. Radiological Equipment.

Chemistry. Organic Coatings. Surface Chemistry. Organic Chemistry. Analytical Chemistry. Inorganic Chemistry. Electrodeposition. Molecular Structure and Properties of Gases. Physical Chemistry. Thermochemistry. Spectrochemistry. Pure Substances.

Mechanics. Sound. Mechanical Instruments. Fluid Mechanics. Engineering Mechanics. Mass and Scale. Capacity, Density, and Fluid Meters. Combustion Controls.

Organic and Fibrous Materials. Rubber. Textiles. Paper. Leather. Testing and Specifications. Polymer Structure. Plastics. Dental Research.

Metallurgy. Thermal Metallurgy. Chemical Metallurgy. Mechanical Metallurgy. Corrosion. Metal Physics.

Mineral Products. Engineering Ceramics. Glass. Refractories. Enameled Metals. Constitution and Microstructure.

Building Technology. Structural Engineering. Fire Protection. Air Conditioning, Heating, and Refrigeration. Floor, Roof, and Wall Coverings. Codes and Safety Standards. Heat Transfer. Concreting Materials.

Applied Mathematics. Numerical Analysis. Computation. Statistical Engineering. Mathematical Physics.

Data Processing Systems. SEAC Engineering Group. Components and Techniques. Digital Circuitry. Digital Systems. Analog Systems. Application Engineering.

- Office of Basic Instrumentation.
- Office of Weights and Measures.

BOULDER, COLORADO

Cryogenic Engineering. Cryogenic Equipment. Cryogenic Processes. Properties of Materials. Gas Liquefaction.

Radio Propagation Physics. Upper Atmosphere Research. Ionospheric Research. Regular Propagation Services. Sun-Earth Relationships. VHF Research. Radio Warning Services. Airglow and Aurora. Radio Astronomy and Arctic Propagation.

Radio Propagation Engineering. Data Reduction Instrumentation. Modulation Research. Radio Noise. Tropospheric Measurements. Tropospheric Analysis. Propagation Obstacles Engineering. Radio-Meteorology. Lower Atmosphere Physics.

Radio Standards. High Frequency Electrical Standards. Radio Broadcast Service. High Frequency Impedance Standards. Electronic Calibration Center. Microwave Physics. Microwave Circuit Standards.

Radio Communication and Systems. Low Frequency and Very Low Frequency Research. High Frequency and Very High Frequency Research. Ultra High Frequency and Super High Frequency Research. Modulation Research. Antenna Research. Navigation Systems. Systems Analysis. Field Operations.

USCOMM-NBS-DC

NBS